The past, present and future of Multi-Scale Modelling applied to wave-structure interaction in Ocean Engineering

V. Sriram[1], Shaswat Saincher[1], S. Yan[2], Q.W. Ma[2]
[1]Department of Ocean Engineering, Indian Institute of Technology Madras.
[2]City, University of London, UK

Abstract

Concepts and evolution of multi-scale modelling from the perspective of wave-structure interaction have been discussed. In this regard, both domain and functional decomposition approaches have come into being. In domain decomposition, the computational domain is spatially segregated to handle the far-field using potential flow models and the near field using Navier-Stokes equations. In functional decomposition, the velocity field is separated into irrotational and rotational parts to facilitate identification of the free surface. These two approaches have been implemented alongside partitioned or monolithic schemes for modelling the structure. The applicability of multi-scale modelling approaches has been established using both mesh-based and meshless schemes. Owing to said diversity in numerical techniques, massively collaborative research has emerged wherein comparative numerical studies are being carried out to identify shortcomings of developed codes and establish best-practices in numerical modelling. Machine learning is also being applied to handle large-scale ocean engineering problems. This paper reports on the past, present and future research consolidating the contributions made over the past 20 years. Some of these past as well as future research contributions have and shall be actualized through funding from the Newton International Fellowship as the next generation of researchers inherits the present-day expertise in multi-scale modelling.

1 Introduction

In this paper, modelling tools and approximations that are in practice for wave-structure interactions (WSI) are discussed. Emphasis is provided for ocean engineering which encompasses offshore and coastal engineering, naval architecture as well as ocean sciences. Thus large time/spatial scale and local time/spatial scales are important. Different modelling aspects based on their level of approximation or theoretical understandings are discussed. This leads to understanding the limitations of the numerical tool, subsequently emphasising how and what to interpret from the results. In recent years, coupling of these standalone tools is being extensively implemented to resolve various levels of the physical process. This is discussed in detail after the brief explanation of the individual tools and how the development took place in each of these modelling efforts.

At present, these numerical models are available as open-source as well as commercial tools using different numerical methods. Thus, said models have varying degrees of approximations in spatio-temporal resolution, stability, accuracy and computational efficiency. Hence, one of the recent efforts in the numerical modelling community is the comparative and benchmarking exercises; this shall also be discussed in the present paper. So the readers can test their own development/existing tools using any of these benchmark tests, available theory and open-source experimental data.

In this paper, apart from providing an overview of the existing tools, a proper classification of the models, their applicability range, computation and physical processes, a thorough literature review on the history of developments are provided. It should be noted that the details of each of the presented models is beyond the scope of this paper and the reader may refer the corresponding literature cited. Through the course of this review, several numerical techniques pertaining to multi-scale modelling shall be covered. However, we refrain from making any best practices recommendations as these strongly depend on the problem at hand and, thus, could be highly subjective. Rather, the aim of this review is to provide the reader with a comprehensive listing of the available methods. This listing has been developed based on the authors' prior experience with multi-scale modelling as well as through a comprehensive review of the state-of-the-art. In the following sections, these mathematical models are discussed with their governing equations to handle physical problems, assumptions, implementation strategies and adopted numerical methods along with their applications. The existing numerical efforts carried out worldwide are provided along with a detailed discussion on numerical model development actualized by the authors' research group that has been supported in-part by the Newton International Fellowship. The remainder of the paper is structured as follows: the spatio-temporal scales associated with various physical processes in ocean engineering along with application-specific levels of approximation necessary in a given model are discussed in **§2**, the depth-resolving Navier-Stokes models along with numerical strategies for solution, wave/current generation and absorption, free-surface tracking as well as turbulence modelling have been discussed in detail in **§3**; potential flow models are introduced in **§3.2**, the depth-averaged Boussinesq-type models are discussed in **§4**, the state-of-the-art in global and regional-scale ocean science multi-scale modelling is presented in detail in **§5**, multi-scale modelling achieved through coupling of different models is discussed in detail from the standpoint of both domain as well as functional decomposition strategies in **§6**, the past and present effort of benchmarking numerical models through comparative studies is reviewed in **§7** and finally the future of multi-scale modelling in WSI is discussed from the standpoint of AI/ML techniques as well as the development of hybrid models for floating renewables in **§8.** The reader will appreciate that significant effort has been made to cover a broad range of modelling techniques in ocean engineering in general and WSI in particular. However, this review is not all-inclusive and hence some fields of research such as hydroelasticity, metocean analysis, wind-wave interaction and phase-averaged wave action modelling could not be included.

2 Different Levels of Approximations

A single numerical tool to address all class of problems in ocean engineering is ideal. However such a model is not possible due to the following reasons: (a) a large sea area, having a large range of spatial and time scales, (b) highly nonlinear wave-structure interaction process (here not only fluid, sometimes the structure can also behave nonlinearly such as vegetation or fenders or hydro-elasticity), (c) waves co-exist with nonlinear currents of various levels, sediment transport and others, (d) viscosity, surface tension and turbulence, (e) two phase (air-sea) or multiphase processes (air-sea-oil or air-sea-sediment), (f) violent wave impacts (during cyclonic storm surges, flooding) and aeration on rubble mound structures, green water shipping and slamming. For these above phenomena, one needs to model large spatial/time scale to capture wave propagation phenomenon as well as resolve small spatial/time scale to understand the wave-structure(-soil) interactions processes. A single mathematical model may not always be a solution for this complex problem. Hence, the researchers have developed various levels of approximations in the mathematical modelling.

The level of approximations in the mathematical modelling are decided based on two guiding principles: (a) which physical process is governing the problem at hand and (b) strive to minimize the computational effort in the resulting numerical algorithm for industrial/practical application by balancing computational efficiency and fidelity. In context to the first principle, the requirement of modelling a physical process is mapped with respect to various applications in Table 1. Table 1 lists various applications that require either large domain or local/small domain modelling.

Table 1. A summarization of the various physical processes and the requirement for them to be modelled for various large and small-scale ocean engineering applications (the information is based on the authors' experience with multi-scale modelling).

			PHYSICAL PROCESSES				
			Surface tension	**Viscous effects and/or turbulence modelling**	**Nonlinearity in fluid**	**Nonlinearity in structure**	**Modelling the air-phase**
APPLICATIONS	**LARGE-SCALE**	**Current/flow-structure interaction**	No	It depends	Yes	No	No
		Wave propagation and interaction	No	It depends	It depends	No	No
		Seakeeping/motion of marine structures	No	It depends	Yes	It depends	No
		Geophysical flows	No	It depends	It depends	No	It depends
		Sediment transport	No	Yes	Yes	No	No
		Wave-breaking	No	Yes	Yes	Yes	It depends
		Aeration dynamics	It depends	Yes	Yes	Yes	Yes
		Wind-wave interaction	It depends	Yes	Yes	No	Yes
		Steep wave and rigid structure	Yes	It depends	Yes	No	No
	LOCAL-/SMALL-SCALE	**Extreme waves and rigid structure**	It depends	It depends	Yes	No	Yes
		Wave-structure-soil interaction	It depends	It depends	Yes	No	No
		Wave-deformable structure-interaction	It depends	It depends	Yes	Yes	Yes
		Current/flow-structure interaction	No	Yes	Yes	It depends	No
		Sediment transport	No	Yes	Yes	No	No
		Wave-breaking	It depends	Yes	Yes	It depends	Yes
		Aeration dynamics	Yes	Yes	Yes	It depends	Yes
		Wind-wave interaction	It depends	Yes	Yes	No	Yes

A typical example for large domain modelling in coastal engineering is wave propagation from offshore to near shore and its interactions with a harbour structure to understand its tranquillity, run-up or inundations. Similar examples from naval architecture and offshore engineering would be ship maneuvering under the action of waves and an offshore wind turbine farm interacting with waves or offshore platform interactions with waves, respectively. For these applications, the physical processes such as surface tension and nonlinearities in structural response are not important. Further, complete physics in modelling the air-sea process is also not required; some empirical treatment would be deemed sufficient. Thus, the full continuity and momentum equations can be simplified based on these approximations.

Similarly, consider an application of small domain modelling, wherein one is interested in quantifying the forces experienced by structures (such as ships, semi-submersible platforms, seawalls, scour around monopiles and jackets etc.) against operating or extreme sea state conditions. In this scenario, normally researchers would carry out the physical model studies in an experimental wave tank. A similar study can be done using numerical modelling based on so-called numerical wave tanks. A numerical wave tank is a numerical tool that could reproduce the experimental facility with a high degree of fidelity. Thus, a detailed physical flow process is realized by solving the continuity and momentum equations, only slightly reducing the physical approximations, nonetheless reproducing the dominating forces as close to reality as possible. For instance, in coastal engineering, surface tension, nonlinearity in structure, sediment to sediment interactions or rigid body interactions (say in a rubble-mound breakwater) can be relaxed without greatly compromising the fidelity of the numerical approximation. Thus, for large scale problems, one can employ various levels of approximations based on the wave characteristics and its applications thus leading to savings in the computational cost. This aspect of modelling is further emphasised by means of a bubble plot in Figure 1 wherein the various environmental aspects in spatial and time scale for mathematical modelling of wave-structure interaction as well as wave-propagation are illustrated.

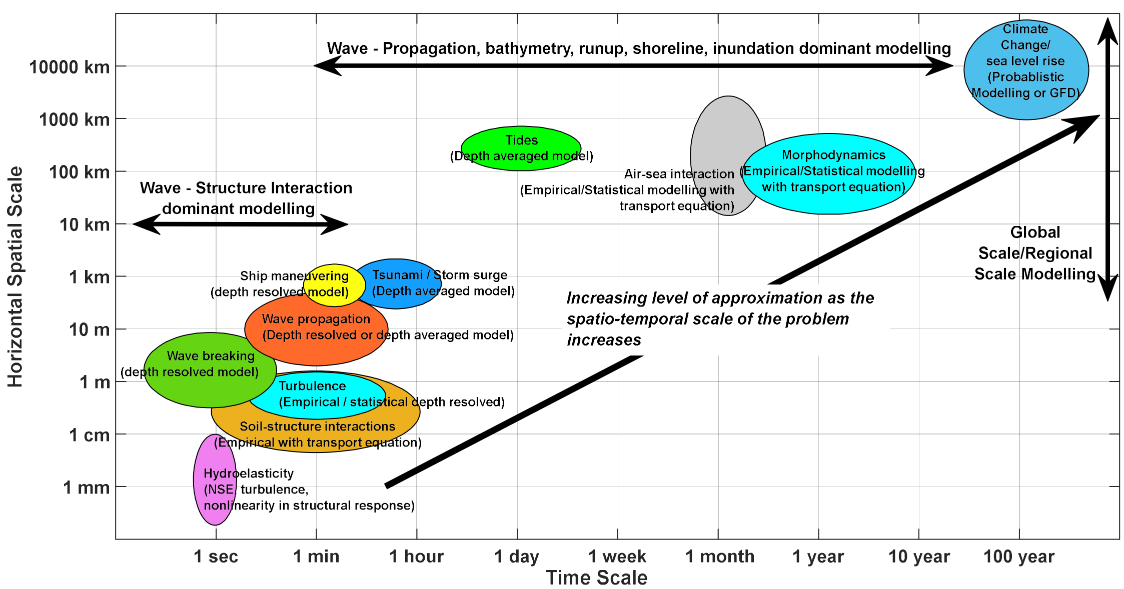

Figure 1. Bubble plot variation to represent the spatio-temporal scales of various physical processes in ocean engineering.

Figure 1 showcase various processes ranging from climate change, sea-level rise, morphodynamics, tides, tsunami/storm surges, wave propagation over varying bathymetry from offshore to their interactions with structures. Each of these cases has a different horizontal spatial scale from 1mm to more than 10,000 km and time scale from less than 1s to 100 years. Further, which type of modelling is dominant and ought to be carried out is also represented (in brackets) in Figure 1, along with global scale or regional scale modelling. The mathematical modelling approximations based on depth averaging can be seen as predominant for increasing large scale problems. This is based on the assumptions of the vertical flow structure. When the vertical flow motion is considered weak or insignificant, then depth averaged horizontal velocities can be adopted. Such classifications of mathematical models are called as depth averaged models and depending upon the approximations adopted in the horizontal velocities different models are available. This will be discussed in the later part of this paper. When the time scale and horizontal spatial scale are small, then the wave-structure interaction becomes dominant; in such cases depth resolving models are normally adopted. This is solved based on Navier-Stokes equations (NSE) with various simplified approximations. Depending upon the application (such as porous-structure, vegetation interactions, hydroelasticity or sediment transport) either microscopic or macroscopic modelling can be adopted within the NS framework to model the structure interaction process. On the other hand, the physical process involved in the ship manoeuvring is of the order of kilometers and minutes at the prototype-scale, however for numerical modelling the same would normally be carried out at a reduced scale using depth resolving models. Hence, for some applications, although the physical process is at a large scale, the numerical simulations are normally carried out at a smaller scale due to computational limitations.

In the past decades, one of the major reasons for resorting to the different physical approximations to model the different scales of the problem was to reduce the computational time. However, this leads to a compromise on the physics of the problem. Figure 2 shows three different broader classifications namely depth averaging, depth resolving and hybrid models. In this broader classification, different governing equations for modelling based on approximations are available, which are currently in practise within the numerical modelling community. The basic modelling task in each case is to solve the continuity and momentum equations for the fluid dynamics problem. However, the modelling complexity increases based on the physical problem being addressed, type of structure (coastal, offshore or marine) and type of sea-state under consideration.

In coastal engineering, the majority of the structures (e.g. breakwaters, sea-walls and pile structures) are fixed or stationary. Then the physical problem to represent is the wave transformation process (i.e., wave shoaling, diffraction, refraction, reflection, wave-overtopping and wave-breaking) and its interaction with the structures. In case of offshore engineering, the structures may be fixed (e.g. offshore wind turbine foundations in < 50 m deep water) or floating (e.g. oil production platforms, floating offshore wind turbines and floating solar arrays). In the latter case, the modelling complexity increases because the fluid flow and structure motion(s) are coupled and thus need to be solved in conjunction; failure to do so would over-predict the hydrodynamic loads. Nonetheless, the overall excursion of an offshore structure is small when compared to marine structures such as a ship or submarine.

For a marine structure, the numerical modelling needs to account for large displacements (e.g. ship maneuvering in waves) thus necessitating large domains and, if the sea-state is violent, also hydroelasticity plays a role (e.g. hull-slamming in violent sea-states). Nonetheless, these scenarios may not always necessitate the NS equations; potential-flow models are a viable alternative as long as the hydrodynamic loads and resulting body motions are properly accounted for. For instance, models based on the Boussinesq equations are quite popular for modelling wave tranquillity and recently, for ship-generated waves.

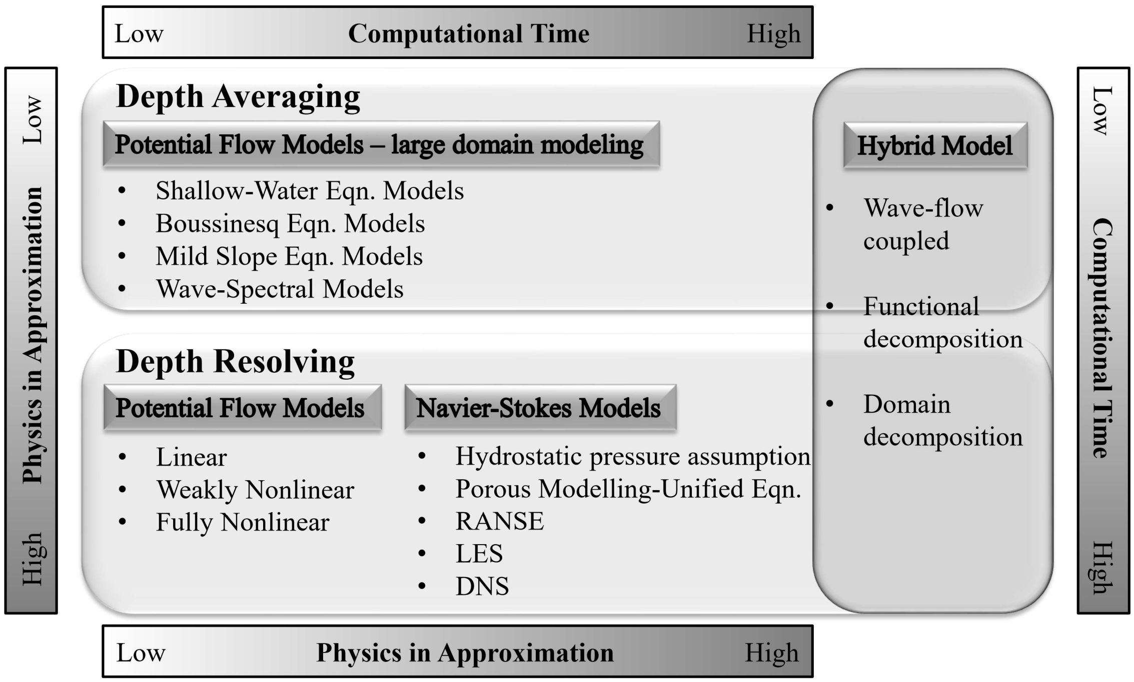

Figure 2. Different modelling strategies characterized by the level of physics approximation and the resulting computational cost.

Various numerical methods are currently in practice to solve a given mathematical model. The numerical methods are broadly classified into strong and weak forms. The traditional methods such as the Finite Difference Method (FDM), the Finite Element Method (FEM), the Boundary Element Method (BEM) and the Finite Volume Method (FVM) as well as modern techniques such as particle/mesh-free methods are being employed in the ocean engineering problems. Mostly, the choice of the numerical methods depends upon the developers and one is not superior to the others as one might expect. Each of these numerical methods has their own advantages and disadvantages, and the overall goal is to reduce or minimize the disadvantages using numerical treatments/algorithms/schemes.

3 Depth Resolving Mathematical Models

In the present section, we review the depth-resolving models. These models are mostly used for the wave-structure interaction problems to estimate the wave loads, wave damping characteristics and motion/structural responses. The problems that are based on small spatial and time scale are normally handled by the depth-resolving approach which models the physical process using a high (spatio-temporal) resolution thus leading to high computational costs.

3.1 Navier Stokes Equations

The Navier-Stokes equations include the equations governing the conservation of mass (termed "equation of continuity" (EOC) for incompressible flows which is in turn a reasonable assumption for WSI) and conservation of momentum. The term "full" indicates the *absence* of simplifying assumptions such as irrotationality, depth-averaging, Reynolds-averaging, two-dimensionality, axisymmetry, single-phase nature of the flow (density is spatio-temporally constant) etc.

3.1.1 Governing Equations

The full Navier-Stokes equations (NSE) governing fluid motion are written here in differential form for the instantaneous velocity field $\vec{V}$:

$$\begin{gathered}\underbrace{\frac{\partial \rho}{\partial t} + \left(\vec{V} \cdot \vec{\nabla}\right)\rho = 0}_{\text{conservation of mass}} \\ \underbrace{\frac{\partial \rho \vec{V}}{\partial t}}_{\text{time}} + \underbrace{\vec{\nabla} \cdot \left(\rho \vec{V} \otimes \vec{V}\right)}_{\text{advection}} = \underbrace{-\vec{\nabla} p}_{\text{pressure}} + \underbrace{\vec{\nabla} \cdot \left(\mu \left\{\vec{\nabla}\vec{V} + \left(\vec{\nabla}\vec{V}\right)^{\mathrm{T}} - \frac{2}{3}\left(\vec{\nabla} \cdot \vec{V}\right)\bar{\bar{\mathbb{I}}}\right\}\right)}_{\text{diffusion}} + \underbrace{\rho \vec{g}}_{\text{gravity}}\end{gathered} \tag{1}$$

where, p is the total pressure, ρ and μ are the density and viscosity respectively, $\bar{\bar{\mathbb{I}}}$ is the identity tensor and $\vec{g}$ is the gravitational acceleration vector. Equation (1) represents the compressible Navier-Stokes equations, however, the compressibility of the fluid may only be important during violent wave-structure interaction at large-scale. For the remainder of the applications, the conservation of mass simplifies to the equation of continuity (EOC): $\vec{\nabla} \cdot \vec{\mathrm{V}} = 0$ which holds for incompressible flow. It is also worth noting that Equation (1) is written for the "instantaneous" velocity-field (Anghan *et al.*, 2019) indicating that $\vec{V}$ is neither time-averaged (RANS) nor spatially-filtered (LES). The fluid properties ρ and μ can be replaced with the mixture properties ρ^* and μ^* to account for the presence of multiple contiguous phases in the domain. Here, advantage is derived from the fact that the phases can be considered as being "individually incompressible" (Saincher and Banerjee, 2018) for most applications which precludes the necessity of solving (say) N sets of the NSE for N phases. This results in the so-called "single-fluid formulation" wherein the entire computational domain is assumed to be filled with a single, albeit, variable-property fluid (Saincher and Sriram, 2022a). It should also be noted that within the single-fluid framework, equation (1) is "conservative" (Saincher and Sriram, 2023) meaning ρ is on the left-hand-side with the time and advection terms. On the other hand, the formulation would be termed "non-conservative" if ρ were on the right-hand-side with the pressure and diffusion terms. The positioning of ρ in the governing equations is immaterial for a single-phase treatment of the NSE (for instance cf. Sriram *et al.*, 2014). The same, however, would have far-reaching consequences for a multiphase framework especially for violent flows involving wave-breaking and/or slamming loads; a conservative formulation is recommended in these cases (Saincher and Sriram, 2023). However, an important limitation of the conservative formulation is that it may lead to the formation of unrealistically large velocities at the interface (Tryggvason *et al.*, 2007) and thus is deemed unnecessary for more benign wave propagation and WSI scenarios. In context to equation (1), it is also worth mentioning that the total pressure p is comprised of static, hydrostatic as well as dynamic contributions; p is not the true pressure but rather a pseudo pressure which satisfies the EOC. The advantage with WSI and ocean engineering problems in general is that the simulation begins from quiescent/calm water conditions which allows for a very accurate "guess" of the initial pressure field using the hydrostatic law. This results in a dynamic pressure field that is very close to the true (say experimentally measured) dynamic pressure, once the hydrostatic contribution has been removed (Saincher and Sriram, 2022a ; 2022b).

3.1.2 Solving the Navier-Stokes Equations

For a given flow problem, the solution variables of interest include the velocity $\vec{V}$ and pressure p. It is characteristic of the incompressible Navier-Stokes equations to *not* have a separate equation for pressure. Owing to this, a majority of incompressible NSE flow solvers are based on a predictor-corrector approach which was pioneered by Chorin (1967); the same is illustrated in Figure 3.

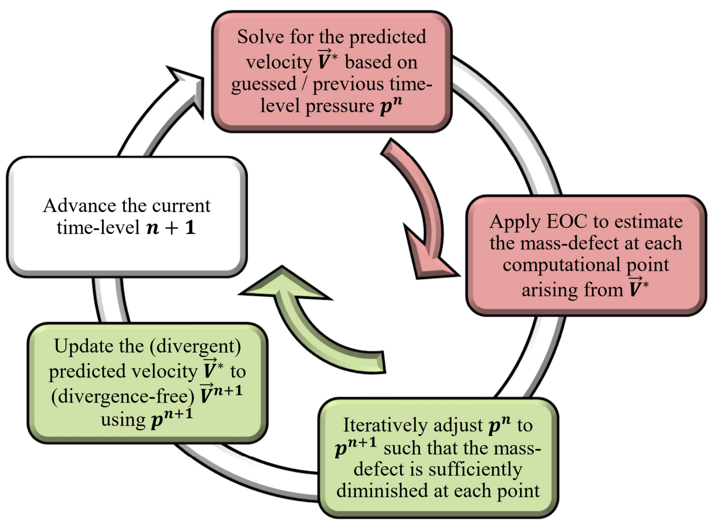

Figure 3. A typical predictor-corrector loop characteristic of projection methods pioneered by Alexandre Chorin in 1967.

At the beginning of the solution, both $\vec{V}^{n+1}$ and p^{n+1} at the current time-level are unknown and the momentum equations are solved for a predicted velocity field $\vec{V}^*$ wherein either:

- the pressure term $\left(-\frac{1}{\rho^*}\vec{\nabla}p\right)^n$ from the previous time-level is considered (Saincher and Banerjee, 2015) or,
- the pressure term is not considered at all which was the case with Chorin's original method (normally adopted in Meshfree methods ; cf. Sriram and Ma, 2021).

At this point, the incompressibility condition $\vec{\nabla} \cdot \vec{V}^{n+1} = 0$ is invoked at the current time-level and the same is split into a mass defect $\vec{\nabla} \cdot \vec{V}^*$ and divergence correction $\vec{\nabla} \cdot \vec{V}'$ contributions. This marks the end of the "predictor-step" (highlighted in red in Figure 3). Following this, the property $\vec{V} = -\frac{\Delta t}{\rho}\vec{\nabla}p$ is invoked to establish a relationship between either $\vec{\nabla} \cdot \vec{V}^*$ and p^{n+1} (Sriram and Ma, 2021) or between $\vec{\nabla} \cdot \vec{V}^*$ and the pressure correction p' (Saincher and Banerjee, 2015). In either case, one ends up with a Pressure Poisson Equation (PPE) which needs to be iteratively solved for p^{n+1} (or an Equation Of Pressure Correction (EOPC) which needs to be iteratively solved for p'). This is oftentimes the most computationally-intensive step in a flow solver. Following solution of the Poisson equation, $\vec{V}^{n+1}$ can be obtained using $\vec{V} = -\frac{\Delta t}{\rho}\vec{\nabla}p$ which marks the end of the "corrector-step" (highlighted in green in Figure 3). The splitting of the solution into predictor and corrector steps is also known as the "projection method" since the pressure is used to project $\vec{V}^*$ onto a space of divergence-free velocity-field which is essentially the Helmholtz decomposition.

Various flow solvers (or so-called "pressure-velocity coupling" schemes) such as SIMPLE, PISO, PIMPLE essentially have the same predictor-corrector constitution but differ with regards to how $\vec{V}^*$ is calculated as well as the number of predictor-corrector cycles per time-step. In fact, regardless of whether $\vec{V}^*$ is computed fully-explicitly or semi-implicitly (because a fully-implicit treatment of the advection term is not possible), the solver still belongs to the SIMPLE class of algorithms (Ferziger *et al.*, 2020). However, some authors also call the fully-explicit category of algorithms "semi-explicit" (Dave *et al.*, 2018 ; Sharma, 2022) owing to the implicit nature of solution of the PPE. It is important to note that, for a given order of time-discretization, the solutions obtained from a fully-explicit or semi-implicit predictor step should be identical. Nonetheless, the semi-implicit treatment would accord further stability to the solution.

In context to WSI, a forward Euler time-discretization and fully-explicit evaluation of $\vec{V}^*$ has been extensively used by the authors (Saincher and Sriram, 2022a ; 2022b ; 2023). From the authors' experience, explicit (forward Euler) time discretization is recommended for waves owing to the hyperbolic nature of solution propagation and a fully-explicit evaluation of $\vec{V}^*$ was found to be sufficient for relatively benign WSI scenarios especially ones that did not involve slamming loads. In fact, it is demonstrated in Saincher *et al.* (2023a ; 2023b) that a fully-explicit evaluation of $\vec{V}^*$ works even in slamming conditions for modest mesh resolutions. Thus, the CFD user ought to make an informed decision whilst selecting the pressure-velocity coupling scheme keeping in mind the trade-off between numerical stability (better for semi-implicit treatment) and computational efficiency (better for fully-explicit treatment). Unfortunately, users of commercial CFD solvers seldom have fully-explicit pressure-velocity coupling available to them and thus alternatively opt for (say) the PISO solver with a Non-Iterative Time Advancement (NITA) option available in ANSYS® FLUENT.

When the predictor and corrector steps are considered in conjunction, say for a 3D flow problem, a single time-step would have one iterative solution loop (for p) in case of a fully-explicit solver and four (for U, V, W, p) in case of a semi-implicit solver. However, our experience suggests that the computational effort required for solving p may sometimes be greater than the three velocity components U, V, W combined. This is primarily because of differences in the rate of convergence which is in turn dependent on the type of boundary conditions involved. The boundary conditions are predominantly Dirichlet in case of velocities which results in predominantly Neumann conditions for the pressure thus leading to an increase in the computational effort for solving the PPE.

3.1.3 Boundary conditions – Wave/Current Generation and Absorption

A prerequisite to accurate WSI simulations in ocean engineering applications is high fidelity wave generation as well as reflection-free absorption of waves/currents in the computational domain. The task of absorption is generally more challenging for WSI simulations involving regular and irregular waves when compared to focusing waves primarily due to the larger number of wave cycles/periods involved in the former case. The task of absorption also becomes complex if currents co-exist with waves. The various methods of wave/current generation and absorption in NSE-based NWTs are mapped against their numerical characteristics in Table 2.

Table 2. Type of wave/current generation and absorption strategies in NSE-based NWTs.

Wavemaker		***U***	***V***	***W***	***p***	***η***
Inflow-boundary		Dirichlet	Dirichlet	Dirichlet	Dirichlet	Dirichlet
Mass-source function		--	--	--	--	Source-term in EOC
Momentum-source function		Source-term in momentum equation			--	--
Internal inlet		--	--	Dirichlet	--	--
Relaxation zone		Dirichlet	Dirichlet	Dirichlet	Dirichlet	Dirichlet
Moving wall	Flap / Piston type Segmented type	Prescribed motion	--	Prescribed motion	--	--
Wave-absorber		***U***	***V***	***W***	***p***	***η***
Outflow boundary		Orlanski / Continuity / Sommerfeld radiation boundary condition				
Sponge-layer		Sink terms in momentum equation			--	--
Relaxation zone		Solution gradually ramped from/to wave theory to/from numerical model				
Moving wall (active absorption)		Prescribed motion	--	Prescribed motion	--	--
Adaptive passive absorption		Adaptively predicted using on-board elevation		Neumann	Neumann	--

With reference to Table 2, the development of "numerical wavemakers" for NSE models was pioneered by Lin and Liu (1998; 1999) wherein the inflow-boundary and mass-source function techniques were proposed. As seen from Table 2, the inflow technique involves a Dirichlet prescription of the wave-induced orbital velocities (predicted from a suitable wave theory) as well as the free-surface elevation at the domain boundary. The present research group has proposed a modified inflow technique to improve the volume-conservation properties of inflow-boundaries, particularly for scenarios involving strong Stokes drift such as steep wave generation in near-shallow water (Saincher and Banerjee, 2017a).

In conjunction with inflow boundaries, the mass-source function technique was also developed which involved the modification of the EOC through the inclusion of a time-varying source term that is in turn proportional to the wave elevation. Wave generation is achieved through periodic ejection/ingestion of water-volume from/into the source region and this offers some advantages over inflow-boundaries. For instance, the only wave characteristic to be input is the time-varying free-surface elevation $\eta(t)$ and thus wave-records from the field could be reproduced. Also, waves reflected from the domain boundaries would not interfere with the wave generation. Nonetheless, the source region itself has several design variables requiring parameterization and, in this context, the authors have proposed guidelines to decide the geometry, placement and strength of the source region based on the relative depth and wave-steepness (Saincher and Banerjee, 2017b). As listed in Table 2, other similar methods have also been proposed such as the internal inlet (Hafsia *et al.*, 2009) and momentum-source function (Choi and Yoon, 2009) techniques. Some researchers have also attempted to directly model piston/flap-type wave-paddle motions into their NWTs using embedded boundary treatment for the solid (cf. fast-fictitious-domain (FFD) based modelling of wave-paddles in Anbarsooz *et al.* (2013)).

However, currently, the most popular technique of numerical wave generation is the so-called "relaxation zones" developed by Jacobsen *et al.* (2012) for OpenFoam®. Here, the solution is spatio-temporally "ramped-up" from wave-theory to NSE before the structure/region of interest and again "ramped-down" from NSE to calm-water conditions after the structure/region of interest. Thus, relaxation zones not only prevent upstream reflection of waves from the far-end of the NWT but also downstream re-reflection of waves reflected off the structure. It is also worth mentioning that relaxation zones in and of itself is a more general concept that has been implemented in hybrid potential theory-NSE models (Agarwal *et al.*, 2022b) as well as in hybrid spectral theory-NSE models (Aliyar *et al.*, 2022).

Apart from relaxation zones, other methods of wave absorption have also been implemented for NSE-based NWTs. For instance, Lin and Liu (1999) employed a radiation/outflow boundary condition for wave absorption at the far-end of the NWT. Outflow boundaries generally implement the Sommerfeld condition (Dave *et al.*, 2018): $\frac{\partial \phi}{\partial t} + C\frac{\partial \phi}{\partial n} = 0$ where ϕ is the property to be effluxed from the boundary, t is time, C is the phase velocity and n points normal to the boundary. The prescription of C is relatively straightforward for "flow problems" making outflow boundaries suitable for tsunamis, tidal flows, scour etc. which involve a dominant current component. Sommerfeld conditions are also suitable for absorbing small-amplitude waves. However, these pose a challenge for absorbing steep waves particularly because C is spatio-temporally variable along the boundary. It has been shown in Dave *et al.* (2018) that improper prescription of C leads to severe (inward) reflections even for free-shear flows.

Self-adaptive wavemaker theory has also been used popularly in both the physical and numerical wave tanks. This method utilizes wavemaker (moving wall) whose motion is specified to generate both the incident waves and an additional wave to cancel the undesirable wave (e.g. the reflected wave from somewhere within the tank). More details can be found in Yan *et al.* (2016). In addition, the same concept of “adaptive absorber” was also used in our recent work on developing a passive wave absorber (Yan *et al.*, 2020). This boundary behaves similarly to the inflow boundary, however the fluid velocity condition is specified by considering its relation with the wave elevation recorded at the boundary. This method does not require the use of the relaxation zone for wave absorption and thus results in a considerable improvement of the computational efficiency. A recent application of the same can be found in Xiao *et al.* (2024).

3.1.4 Free surface capturing/tracking

A majority of ocean engineering problems involve waves and/or other flows such as bores, hydraulic jumps, etc. which necessitates computing the topology of the free-surface. In reality, the free-surface marks a discontinuity between two media (say air and water) and thus acts as an interface. The numerical algorithms for computing the interfacial topology can be broadly classified into interface-tracking and interface-capturing techniques. In the former category of algorithms, the free-surface is modelled as a boundary and is tracked by updating the mesh as the solution progresses. In the latter category, the free-surface evolves spatio-temporally within a fixed domain wherein the interface is identified by an indicator function. Interface-capturing algorithms are obviously more advantageous (especially for violent flows involving complex interfacial deformation such as overturning and aeration) and thus have been extensively employed in NSE-based flow solvers; the same have been listed in Table 3.

As evidenced from Table 3, the interface-capturing algorithms can be further classified based on the technique used for interface identification (“reconstruction”) and advection. The interface identification techniques differ based on the type of indicator function used (volume fraction or level-set function) as well as whether the identification itself is geometric in nature or not. The level-set method and high-resolution schemes such as the Compressive Interface Capturing Scheme for Arbitrary Meshes (CICSAM) are algebraic in nature in that they do not involve explicit geometrical computations of the placement (or advection) of the interface within the domain. In comparison, geometric methods such as the Piecewise Linear Interface Calculation-Volume Of Fluid (PLIC-VOF) and Moment Of Fluid (MOF) are higher fidelity in that the interfacial coordinates are geometrically computed subject to conservation of the primary phase volume in each cell.

Volume conservation is intrinsic for geometric VOF methods and also for single-phase meshfree methods such as the Improved Meshless Local Petrov-Galerkin method with Rankine source function (IMLPG_R). This is not the case for algebraic VOF schemes or the level-set method where additional numerical treatment is necessary to achieve volume conservation. This has been comprehensively demonstrated by the present authors (Saincher and Sriram, 2022a) and others (Anghan *et al.*, 2021 ; Arote *et al.*, 2021) wherein a material redistribution algorithm originally developed for geometric VOF (Saincher and Banerjee,

2015) has been shown to dramatically improve the volume conservation properties of algebraic VOF schemes.

Similarly, interfacial diffusion is intrinsic for algebraic VOF as well as level-set methods. This could be mitigated to some extent using operator-split/direction-split advection as doing so would eliminate multi-fluxing errors (Saincher and Sriram, 2022a). Whilst algebraic VOF techniques are indeed capable of capturing large-scale interfacial segregation in WSI problems (Saincher *et al.*, 2023a), small-scale droplets and bubbles would still diffuse upon separation from the parent phase. This diffusion seldom contributes to the hydrodynamics in a WSI simulation and, in fact, provides numerical stability to the solution. Conversely, droplets/bubbles separating from the parent phase would never dissipate in geometric VOF and thus excessive interfacial fragmentation might, in fact, lead to solver instability.

Table 3. Various interface-capturing algorithms developed for NSE-solvers; cf. nomenclature for the abbreviations.

Authors	**Algorithm**	**Interface identification**	**Interface advection**	**Interface diffusion**	**Volume conservation**	**Mesh**
O'Shea *et al.* (2014)	NFA	Geometric VOF	Unsplit Eulerian	Zero	Intrinsic	Cartesian
Sriram *et al.* (2014)	IMLPG_R	MPNDAF	Lagrangian	Zero	Intrinsic	--
Saincher and Banerjee (2015)	Redistribution-based PLIC-VOF	Geometric PLIC-VOF	Operator-split Eulerian	Zero	Intrinsic	Cartesian
Bihs *et al.* (2016)	REEF3D	Level-set	Unsplit Eulerian	Intrinsic	Extrinsic	Cartesian
Zinjala and Banerjee (2016)	LEAS-MOF	Geometric MOF	Lagrangian-Eulerian	Zero	Intrinsic	General Polygonal
Zinjala and Banerjee (2017)	RMOF	Geometric MOF	Lagrangian-Eulerian	Zero	Intrinsic	General Polygonal
Anghan *et al.* (2021)	MSTACS	Algebraic VOF	Unsplit Eulerian	Intrinsic	Extrinsic	Cartesian
Arote *et al.* (2021)	SAISH	Algebraic VOF	Unsplit Eulerian	Intrinsic	Extrinsic	Cartesian
Saincher and Sriram (2022a)	OS-CICSAM	Algebraic VOF	Operator-split Eulerian	Intrinsic	Extrinsic	Cartesian

3.1.5 Turbulence Modelling

Ocean engineering problems involve flow of sea-water which has a kinematic viscosity of $\nu \sim 1e-06\ \mathrm{m^2/s}$. The corresponding Reynolds number $\mathrm{Re} = \mathcal{V} \cdot \mathcal{L}/\nu$ would typically be $O(10^6)$ even if the characteristic velocity ($\mathcal{V}$) and length ($\mathcal{L}$) are $O(1)$, that is, at model-scale. This is generally the case since the Froude-law is invoked for scaling based on the fact that gravity is the dominant restoring force in ocean engineering applications. As a consequence, most scenarios being simulated are not laminar and some form of modelling may be required to account for the additional viscous effects near the structure. Some of the typical applications necessitating turbulence modelling include:

- Wave/tsunami interactions with vegetation: turbulence-induced viscous effects arising from flow separation need to be accounted for to correctly estimate energy attenuation.
- Response of floating bodies: failing to account for viscous effects within the boundary layer may result in over-prediction of the motion response.
- Resistance of marine vessels in waves/calm water: failing to account for viscous effects within the boundary layer may result in under-prediction of resistance.

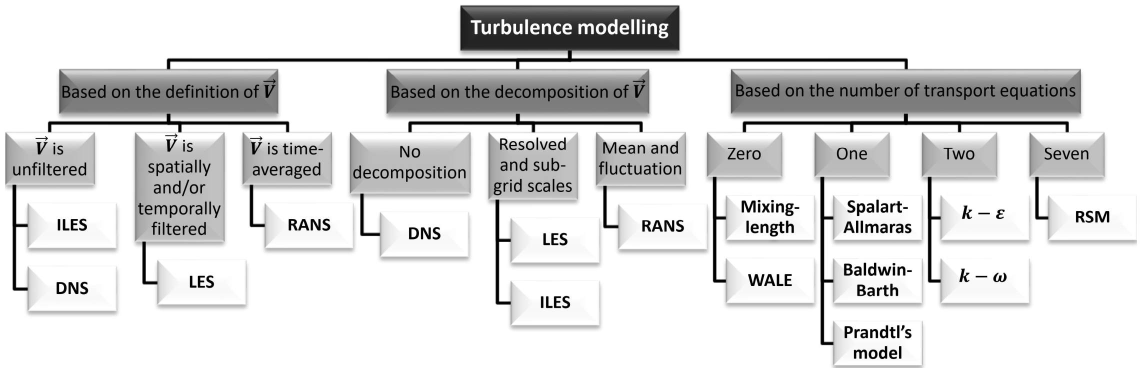

Figure 4. An illustration of the different means to categorize various strategies to model turbulence in depth-resolving models; cf. nomenclature for the abbreviations.

Several popular methods have been developed for modelling turbulence in NSE-based solvers; some have been integrated with self-developed codes by the present research group. There exist different means of classifying turbulence modelling strategies for depth-resolving methods; the same are depicted in Figure 4. In conjunction with Figure 4, the momentum equation (1) is also re-written to account for turbulence modelling:

$$\underbrace{\frac{\partial \vec{\boldsymbol{V}}}{\partial t}}_{\text{time}} + \underbrace{(\vec{\boldsymbol{V}} \cdot \vec{\nabla})\vec{\boldsymbol{V}}}_{\text{advection}} = \underbrace{-\frac{1}{\rho^*}\vec{\nabla}\boldsymbol{p}'}_{\text{pressure}} + \underbrace{\frac{1}{\rho^*}\vec{\nabla} \cdot \left((\mu^* + \boldsymbol{\mu_t})\vec{\nabla}\vec{\boldsymbol{V}}\right)}_{\text{diffusion}} + \underbrace{\vec{g}}_{\text{gravity}} \tag{2}$$

where, p' is the modified pressure which includes the normal components of the Reynolds or Sub-Grid-Scale (SGS) stress tensor and μ_t is the turbulent viscosity; the terms modified/introduced by turbulence modelling have been highlighted in bold. In context to equation (2) and Figure 4, $\vec{V}$ can be unfiltered, spatio-temporally filtered or time-averaged. The filtering and time-averaging operations are essentially decompositions of the unfiltered velocity and thus, once performed, information about the instantaneous velocity field is invariably lost. For instance, the $\vec{V}$ field obtained following solution to the RANS equations is time-averaged and thus, (temporal) fluctuations in $\vec{V}$ do not represent fluctuations in the instantaneous field. Only the effect of the true fluctuating field on $\vec{V}$ is modelled through the eddy viscosity μ_t.

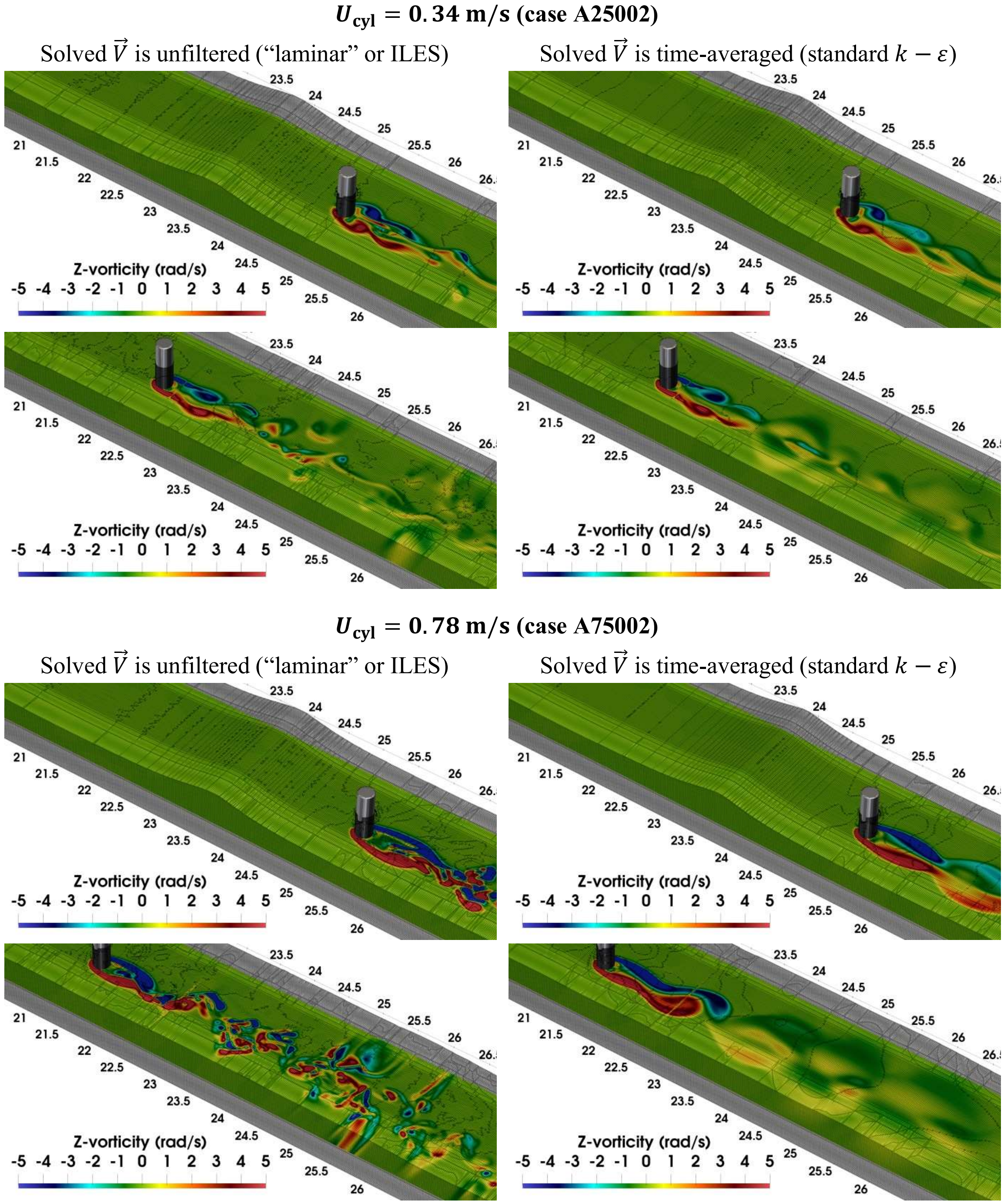

Figure 5. The vorticity field $(\vec{\nabla} \times \vec{V})$ generated by a moving cylinder interacting with a focusing wave (Sainplace Sainicher and Sriram, 2022b); note the change in the nature of the solution based on the definition of $\vec{V}$. The cylinder moves from bottom-right to top-left.

This important aspect is illustrated in Figure 5 wherein vortices shed by a moving cylinder interacting with focusing waves are shown (adapted from Saincher and Sriram (2022b)). The same problem has been simulated first using unfiltered NSE (a "laminar" solver) and then using time-averaged NSE (a RANS solver based on standard $k - \varepsilon$ (SKE)). The aforementioned loss of information regarding the true fluctuating velocity field is readily

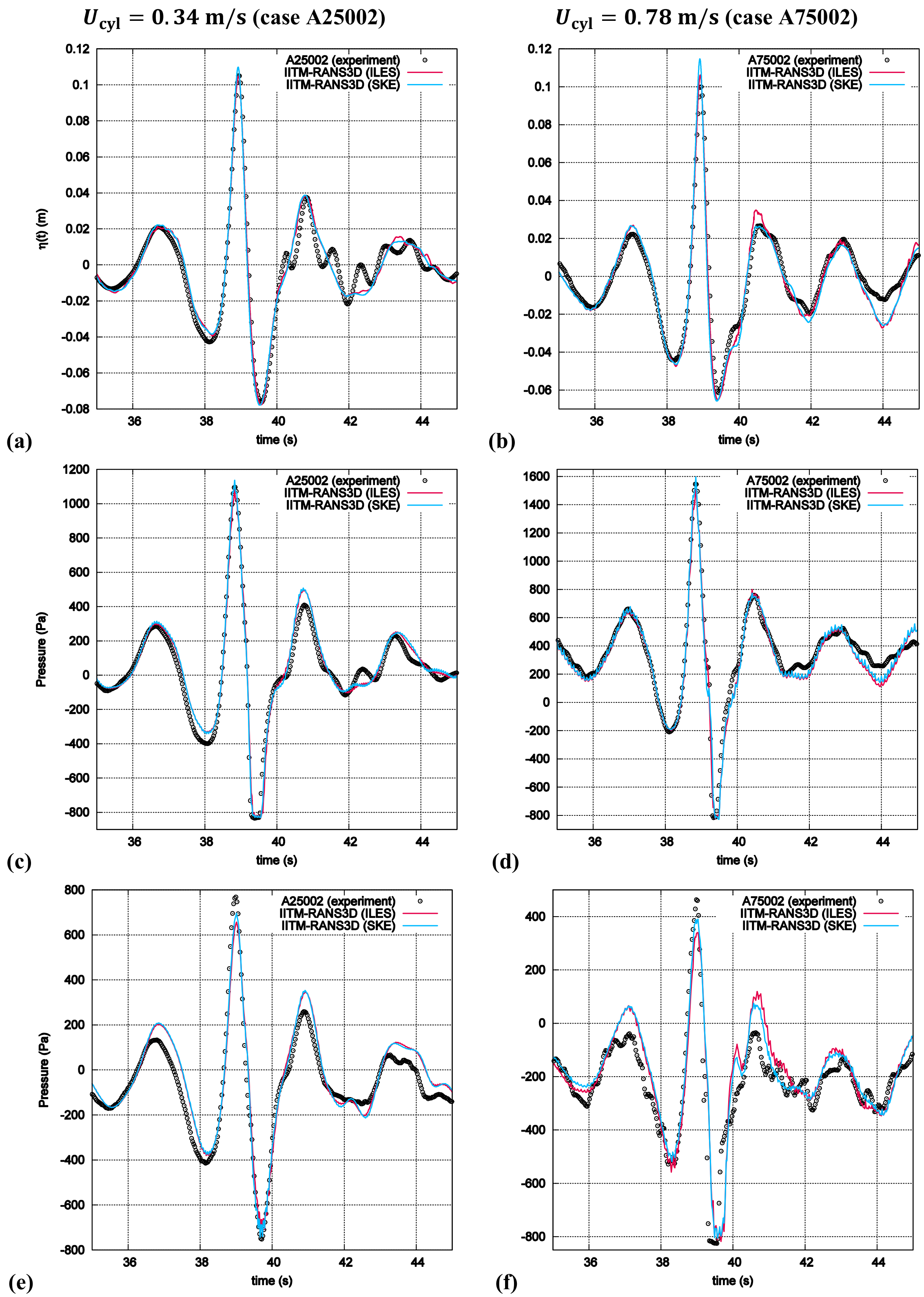

Figure 6. Time-histories of free-surface elevation ($\eta(t)$) and pressure ($p(t)$) corresponding to a moving cylinder interacting with focusing waves (Saincher and Sriram (2022b)): (a,b) $\eta(t)$ variation in-line with the center of the moving cylinder and $p(t)$ variation just below the SWL at the (c,d) forward and (e,f) rear stagnation points.

apparent from Figure 5; the vorticity field is "instantaneous" in both cases. It should also be noted that the so-called "laminar" solver is a misnomer as it simply refers to solving the NSE without any turbulence modelling. In this regard, the laminar approach is not a Direct Numerical Simulation or DNS (since no attempt is made to resolve the Kolmogorov scales) but rather a form of Implicit Large Eddy Simulation or ILES (wherein the discretization errors would mimic SGS modelling (Rodi *et al.*, 2013)). Having said that, figure 5 indicates that the laminar solver captures more "turbulence" than the actual turbulence model!
In addition to the above qualitative assessment, it is also important to quantify the impact of turbulence modelling (or lack thereof) on quantities of engineering importance. In order to do this, the time-variation of the free-surface elevation measured in the vicinity as well as pressure measured on the surface of the moving cylinder is reported in Figure 6 for both ILES and SKE simulations. It can be seen that ILES and SKE results are practically identical for the lower towing speed. This is corroborated by the vorticity fields (for $U_{\mathrm{cyl}} = 0.34\ \mathrm{m/s}$) reported in Figure 5. For the higher towing speed, the SKE results show a closer agreement with experiments in terms of both $\eta(t)$ variation as well as pressure at the rear stagnation point. However, the improvement gained from turbulence modelling in this case is not dramatic (even though the computed vorticity fields are dramatically different). The findings are in line with conclusions drawn from the ISOPE 2020 comparative study which was based on the same experimental dataset (Agarwal *et al.*, 2021a).

The necessity and nature of turbulence modelling depends on the nature of the problem itself and oftentimes the fidelity of the solution/simulation (against experiments) depends on the expertise of the CFD practitioner (this is later discussed at length in §7 on comparative numerical studies). One is not only required to assess the need of a turbulence model but also the impact of a particular model on the solution. Considering a wave-floating structure interaction problem as an example, a need for turbulence modelling may arise due to an over-prediction of the angular acceleration of the body by a laminar model. If RANS-based turbulence modelling is introduced to supplement the viscous damping in the near-field of the body, the same may also negatively impact the simulation through unwanted damping of the incident waves. In such a case, the unwanted damping could be mitigated by:

- Stabilizing the unbounded growth of μ_t using limiters (Larsen and Fuhrman, 2018).
- Increasing advection using higher-order upwind schemes (Saincher and Sriram, 2022b).
- Increasing advection using conservative NSE formulations (Saincher and Sriram, 2023).
- Switching to a less empirical model such as WALE (zero-equation model with a single model constant) for computing μ_t (Rodi *et al.*, 2013).

The above discussion indicates that there exist multiple solutions to a given problem and there is a general consensus that the simplest models also prove to be the most robust. Taking into account the strongly empirical nature of turbulence modelling in general (RANS in particular), a modestly accurate albeit robust model applicable to several problems should be preferred over a heavily calibrated model that works perfectly albeit only for a single problem. Further, turbulence model should only be employed for the practical problems in need and not for all scenarios.

3.1.6 Numerical Methods

In addition to the algorithms used for pressure-velocity coupling, interface capturing and turbulence modelling, the flow solver is also comprised of spatio-temporal discretization schemes as well as linear equation systems solvers. Both categories of algorithms directly impact the accuracy and stability of the flow solver.

Some of the popular discretization schemes that have been widely implemented for ocean engineering problems are now discussed in context to the momentum equation (1) and Table 4. Discretization of the time-term can be carried out either using Linear Multi-step Methods (LMMs) or Runge-Kutta (RK) methods. These two categories of methods can be further classified into explicit and implicit schemes. Explicit LMMs are also known as the Adams-Bashforth Methods (ABMs) whilst implicit LMMs are known as Adams-Moulton Methods (AMMs). As the name suggests, LMMs build accuracy by storing the flow solution across multiple time-levels such that a first-order LMM would require an existing flow-field solution from one time-level, a second-order LMM would necessitate solutions from two time-levels and so on. Owing to the requirement of an existing flow-field solution, LMMs $> \mathcal{O}(1)$ are not "self-starting" and some complexities exist in implementing these methods for variable time-steps. Moreover, the region of stability of LMMs shrinks with increasing order of accuracy (Drikakis and Rider, 2005). Nonetheless, a key advantage of LMMs is that the per-time-step computation effort does not increase with increasing order of accuracy; only the storage requirements increase.

On the other hand, RK methods divide a single time-step into a number of intermediate steps with all intermediate velocity fields made divergence-free; only the most recently known velocity field is necessary for a given intermediate step. Given this characteristic, RK methods are self-starting and automatically account for variable time-steps. However, the fact that the predictor-corrector loop (cf. Figure 3) is executed multiple times within a time-step introduces a unique set of merits and shortcomings. The chief merit is the numerical stability which, unlike LMMs, increases with increasing order of the method. Another merit over LMMs is that storage requirements do not increase with increasing order. The chief shortcoming associated with RK methods is that each intermediate step entails a computationally expensive solution of the elliptic PPE or EOPC; per-time-step computation effort thus increases with increasing order. Referring to Table 4, it is seen that a number of NSE algorithms implement explicit time-integration (ABM or Total Variation Diminishing-RK (TVD-RK)) which is suitable given the hyperbolic nature of wave propagation. In cases where a greater amount of numerical stability is desired, say conservative NSE formulations for violent WSI (Benoit *et al.*, 2023) authors opt for AMM rather than TVD-RK. This is probably because the additional linear equation systems encountered for AMM (one system for each component of $\vec{V}$) is parabolic and less expensive to solve than the elliptic PPE/EOPC encountered multiple times within a time-step in the case of TVD-RK. It is also possible that very high-order AMMs might lead to dispersive (phase) errors in wave-propagation.

Table 4. A summary of the various discretization methods and linear equation system solvers implemented for NSE algorithms applied to ocean engineering problems reported in the literature; cf. nomenclature for abbreviations. (✘: data unavailable)

Authors	**Time**	**Momentum Advection**		**Pressure**	**Diffusion**	**PPE/EOPC**
		Scheme	**Treatment**			
Sriram *et al.* (2014)	ABM1	Lagrangian	--	SFDI	SFDI	GMRES
Bihs *et al.* (2016)	TVD-RK3	WENO	Non-conservative	✘	✘	BiCGStab
Xie and Stoesser (2020)	AMM1	Second-order TVD	Conservative	CD2	CD2	ADI / BiCGStab
Agarwal *et al.* (2021b)	ABM1	Lagrangian	--	SFDI	SFDI	BiCGStab
Anghan *et al.* (2022)	ABM2	Blended FOU-FiOU	Non-conservative	CD2	CD4	GSSOR
Saincher and Sriram (2022b)	ABM1	Blended FOU-FiOU	Non-conservative	CD2	CD2	GSSOR
Benoit *et al.* (2023)	AMM1	Slope-limited SOU	Conservative	CD2 with third-order numerical smoothing		GMRES
Saincher and Sriram (2023)	ABM1	Blended FOU-FiOU	Conservative	CD2	CD2	GSSOR

In addition to time-integration, the numerical schemes chosen for momentum advection, pressure and diffusion terms as well as the linear systems solver chosen for solving the pressure field also play a key role in deciding the robustness and accuracy of NSE solvers. In context to the discretization of the pressure and diffusion terms, second-order central differencing (CD2) suffices for most scenarios and is thus the most widely used (cf. Table 4). However, recent studies involving DNS of marine outfalls have instead implemented fourth-order central differencing (CD4) for higher resolution treatment of the diffusion term (cf. Anghan *et al.*, 2022). It should also be noted that CD4 treatment of the pressure gradient does not dramatically improve the accuracy of a solver and should rather be avoided to save computational effort (Tafti, 1996).

Numerical formulations of the NSE inherently contain some form of numerical diffusion. In context to ocean engineering applications, this diffusion gets manifested as a gradual reduction in wave-height (Saincher and Banerjee, 2017). Whilst the numerical diffusion can be arrested through mesh refinement, a more computationally efficient way to do this (especially for mesh-based Eulerian solvers) is by increasing the order of advection discretization. However, computational efficiency does not translate to a straightforward implementation, especially for multiphase solvers. Implementation of a high order advection scheme in its "pure form" leads to severe dispersion errors in regions of sharp velocity gradients which, in case of waves, prevail at the air-water interface; the consequence is unphysical deformation of the generated waves. This can be corrected by either using inherently bounded schemes such as WENO (Bihs *et al.*, 2016) or blended schemes where (say) only 50% of the advected momentum is estimated using the high-order scheme, the rest being estimated using FOU (Saincher and Sriram, 2022b). For more violent scenarios involving wave-breaking and/or wave-slamming, a higher order treatment of advection may not be sufficient and rather the correct amount of advection being attributed to each fluid-phase needs to be ensured. This is where conservative NSE formulations come into picture wherein ρ^* is shifted to the left-hand-side of equation (1) with the time and advection terms. It has been recently demonstrated by the authors that conservative NSE solvers are necessary for correctly capturing the topology of waves overturning over a long distance; such as solitary waves breaking over a beach/shallow water (Saincher and Sriram, 2023). It is worth mentioning that conservative NSE formulations strongly and consistently couple mass and momentum transport (cf. the discussion on mass inconsistency in Saincher and Sriram (2023)) and thus momentum advection is more strongly governed by material transport (owing to the $1:800$ density ratio between air and water) rather than the momentum advection scheme itself (Bussmann *et al.*, 2002). This makes conservative NSE a suitable alternative to high-order advection schemes for arresting wave-damping in non-violent/moderately violent WSI scenarios.

For rigid structures, one can incorporate this in the computational domain and solve the interaction problems as shown in Figure 5. For elastic and floating structures, a separate equation of motion will be solved to understand the fluid-structure interaction process, see, Sriram and Ma (2012), Rijas *et al.* (2019) and Vineesh and Sriram (2022). In the case of modelling porous/vegetation structure interactions with waves, one can adopt microscopic or macroscopic approaches. The macroscopic approach is commonly adopted due to the computational advantages as well as in terms of requirement for physical process (see, Divya and Sriram (2020)). For modelling the porous/vegetation structure interaction with waves, additional resistance terms such as the: (a) linear drag coefficient representing the laminar flow, (b) non-linear drag coefficient representing the turbulent flow, (c) coefficient for the transitional flow and (d) virtual mass coefficient for inertia terms were incorporated in the governing equations. The numerical studies on the wave porous structure can be carried out in two different ways:

(i) Coupling of pure fluid and porous flow equations, in which the fluid flow is solved using the NSE and porous flow with different porous flow model, following which the interface was coupled by matching the flow properties. Such coupling can be explicit, implicit or iterative in nature.

(ii) Based on unified or single governing equations to model both porous structure and fluid flow. In the microscopic approach, the aim is to capture detailed flow physics, directly resolved by the NSE (see Xie and Stoesser (2023)).

Apart from mesh based approach in solving the NS, mesh-free or particle methods are quite popular and further developments are actively being carried out. These developments have been the topic of many recent review papers such as Luo *et al.* (2021), Sriram and Ma (2021), Lind *et al.* (2020) and references therein. However, the acceptability of the mesh-free methods or particle methods for industry and practical applications in the projects are not matured compared to mesh-based methods. The consolidation of the work carried out by the authors with regards to the mesh-free method based on Meshless Local Petrov Galerkin Method (MLPG) has been reviewed in detail in Sriram and Ma (2021) and shall not be repeated here for the sake of brevity. Further, an important relation between the widely popular Smoothed Particle Hydrodynamics (SPH), Moving Particle Semi-Implicit Method (MPS) and MLPG was established. However, as this special issue concerns the Newton fellowships, a flow chart of development has been reproduced for completeness as shown in Figure 7.

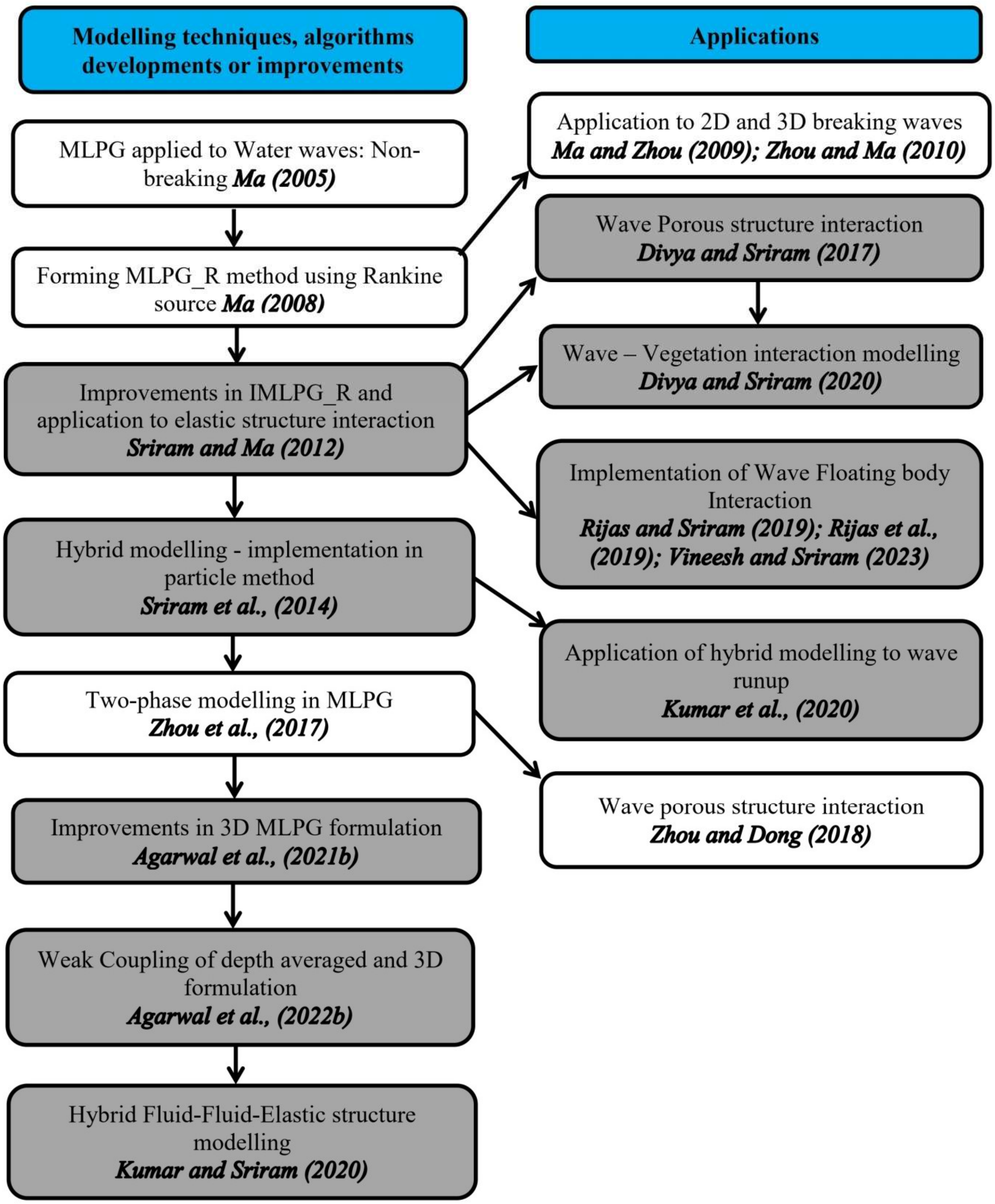

Figure 7. Summary of the history of the development of the Meshless Local Petrov Galerkin method (MLPG) and its application in Ocean Engineering (revised and updated from Sriram and Ma, 2021). Grey shaded boxes are development with partial or full support from the Newton fellowship.

3.2 Potential Flow Theory

The fully nonlinear potential flow theory (FNPT) has significantly matured in today's context and is being extensively used by both researchers as well as industry. The methodology was pioneered by Longuet-Higgins and Cokelet (1976) using a mixed Eulerian and Lagrangian approach. The simulation of nonlinear waves using FNPT can be carried out either by fully discretising the domain and then solving the Laplace equation using numerical approaches (like FEM, BEM and so on) or by obtaining the solution of the Laplace equations using spectral, Eigen function or Fourier methods. In the former case, the computational effort would be quite significant when one extends the method to 3D, however, the advantage is that one can simulate waves interacting with any arbitrarily complex structure. In the latter approach, the computational effort is lesser in comparison and such methods are largely employed for simulating the fully nonlinear waves. Dommermuth and Yue (1987) and West *et al.* (1987) proposed an attractive fast convergence, high accuracy and fast resolution properties-based higher order spectral (HOS) method. These fast methods of computation are very useful for calculating the long-time evolution of nonlinear waves and can be used as an input for the numerical models based on the NS equations. A detailed review of these models can be found in Kim *et al.* (1999) and in Ma (2008) and references therein. Normally, the FNPT-based models are quite effective in reproducing the extreme steep non-breaking waves, however, once the wave begins to overturn (the crest becomes vertical), the simulation crashes (Mohanlal, 2023). For some models, the crash may be delayed up to the point when the overturning crest hits the free-surface (Grilli *et al.*, 2001). Naturally, the conventional FNPT models cannot handle wave-trains in which multiple breaking events occur in succession (over a period of time). In order to overcome these effects and carry out the simulations of overturning waves for a longer duration, researchers employ empirical treatment such as eddy viscosity models to incorporate breaking effects (Tian *et al.* (2010), Barthelemy *et al.* (2018), Sieffert and Ducrozet (2018), Hasan *et al.* (2019)). Very recently, Mohanlal (2023) has developed a FNPT model to handle multiple depth-limited two-dimensional breaking events in irregular sea-states, steepness-limited breaking of two-dimensional focusing waves as well as depth-limited breaking of regular waves over three-dimensional bathymetry. In their model, incipient breaking is detected based on whether the ratio of the orbital velocity to the wave-celerity exceeds a given threshold. Following detection, the energy of the over-turning wave is dissipated through an absorbing/damping surface pressure term introduced into the dynamic free-surface boundary condition (Grilli and Horrillo, 1997). It is worth mentioning that the wave generation techniques discussed in Table 2 in context to the NS models can also been incorporated in the FNPT models, mostly using moving wall, relaxation zone and/or prescribing inlet wave characteristics.

4 Depth-averaged Mathematical Models

The depth-averaged models are governed by the Boussinesq Equations (BSNQE), the Green-Naghdi equations, the Korteweg-De Vries (KdV) equation or the Shallow-Water Equations (SWE). These models are based on an assumption that the horizontal velocities (in the shoreward and longshore directions) are uniform or varying over the water column. A summary of the depth-averaged mathematical models is provided in Table 5; it can be appreciated that the models are being actively developed since the 1960s. In some of the models, the approach is based on the notion of a uniform horizontal velocity, which is a characteristic of long-wave-induced orbital kinematics, the baseline models are limited to shallow-water. It is evidenced from Table 5 that the research effort has been driven by the need to expand the applicability of these models to deep-water ($kd \geq \pi$). This was achieved through various means such as:

- replacing the depth-averaged velocity by velocity defined at an arbitrary depth to act as the velocity variable (Nwogu, 1993),
- improving the dispersion characteristics through modification of the governing equations (Beji and Nadaoka, 1996) and
- piecewise integration of the momentum equations over multiple layers yielding separate velocity profiles within each layer (Lynett and Liu, 2004a).

Table 5. A summary of various depth-averaged mathematical models developed for wave-propagation reported in the literature; cf. nomenclature for abbreviations.

Authors	**Model**	**Numerics**	**Waves**	**Breaking**	**Multilayer**
Peregrine (1967)	Nonlinear BSNQE for varying depth	FDM	Solitary	No	No
Green and Naghdi (1976)	Wave propagation in variable depth (rotational)	Analytical	--	No	No
Madsen *et al.* (1991)	Linear dispersive BSNQE for deep water	FDM	Regular, Bichromatic ($1.95 \leq kd \leq 2.72$)	No	No
Nwogu (1993)	Nonlinear BSNQE with velocity at arbitrary depth	FDM	Regular, Irregular ($0.44 \leq kd \leq 3.13$)	No	No
Wei *et al.* (1995)	Fully nonlinear BSNQE for varying depth	FDM	Solitary, Undular bore	No	No
Beji and Nadaoka (1996)	Improved BSNQE for varying depth	FDM	Regular ($0.47 \leq kd \leq 1.91$)	No	No
Lynett *et al.* (2002)	Fully nonlinear BSNQE	FDM	Regular, Solitary ($kd = 0.14$)	Yes	No
Madsen et al. (2002)	Fully nonlinear BSNQE	FDM	Solitary, Regular ($0.65 \leq kd \leq 2\pi$)	No	No
Lynett and Liu (2004a)	Multi-layer BSNQE	Analytical	Regular ($\pi \leq kd \leq 8\pi$)	No	Yes
Lynett and Liu (2004b)	Multi-layer BSNQE	FDM	Regular, Solitary, Landslide ($0.70 \leq kd \leq 9.00$)	No	Yes
Sitanggang and Lynett (2005)	Fully nonlinear BSNQE	FDM	Gaussian hump, Solitary, Regular ($kd = 1.27$)	No	No
Shi et al. (2012)	Fully nonlinear BSNQE	FDM + FVM	Regular, Irregular, Solitary ($0.36 \leq kd \leq 0.78$)	Yes	No
Yang and Liu (2020)	Wave-current model for varying depth based on Euler equations	Galerkin, Subdomain methods	Regular, Focusing + sheared current ($1.00 \leq kd \leq 22.0$)	No	No
Agarwal *et al.* (2022a)	Fully nonlinear BSNQE	FEM	Regular, Solitary, Ship-generated ($0.73 \leq kd \leq 1.92$)	No	No

These models have been employed to address larger-scale spatial ($\sim$km) and temporal ($\sim$min) processes in ocean engineering such as ship-generated waves in bays and inland waterways (cf. Agarwal *et al.*, 2022a). The depth-averaged models are widely used in the industry for waves and current hydrodynamics with models capable of handling interactions between waves and sheared currents being recently proposed by Yang and Liu (2020). Whilst the BSNQE-based models are based on irrotational and inviscid assumptions, turbulence and wave breaking have also been treated using the empirical approaches (Lynett *et al.*, 2002 ; Shi *et al.*, 2012). The BSNQE-based models have also been used for coupling with NS equations-based models to minimize the computational time (cf. Agarwal *et al.*, 2022b and references therein). It is worth mentioning that the different approaches of wave-generation/absorption discussed in Table 2 in context to the NS models are also applicable to depth-averaged models except the moving wall approach. It is also worth noting that the present review only aims at providing a brief overview of the development of BSNQE-type models for the sake of completeness in context to multi-scale modelling and is by no means all-inclusive. The reader is referred to Brocchini (2013) for a detailed review.

5 Regional and global-scale modelling in Ocean Sciences

If one refers back to the spatio-temporal scale classification of physical processes and models in Figure 1, it is seen that the BSNQE-type depth-averaged models belong in the $\sim 1\ \mathrm{km}/1\ \mathrm{h}$ category. Whilst this is considerably "large-scale" compared to the depth-resolved models ($\sim 1\ \mathrm{m}/1\ \mathrm{min}$), the depth-averaged models are also considerably "small-scale" to regional and global-scale models ($\sim 10^3\ \mathrm{km}/1\ \mathrm{ka}$) that are typically applied in ocean sciences. Both regional and global-scale simulations in ocean sciences have been traditionally and fundamentally based on the concept of multi-scale modelling. Having said that, popular ocean-science models are generally based on RANS-type momentum equations; multi-scale modelling is seldom achieved through the inclusion of potential theory or Laplace equations. This is primarily because such models belong to the class of Ocean General Circulation Models (OGCMs) wherein the assumptions of zero viscosity and vorticity need to be relaxed. A summarization of the state of the art in the development of regional and global-scale ocean models is provided in Table 6.

Table 6. A summary of various regional and global ocean models developed for various ocean science applications reported in the literature; cf. nomenclature for abbreviations.

Authors	Model	Mathematical framework	Scales		Application
			Spatial	Temporal	
Bryan (1968)	--	NSE in geodetic coordinates (Hydrostatic, Boussinesq approximation, turbulent viscosity)	Indian Ocean	30 years	Circulation of the World Ocean
Bleck and Boudra (1981)	--	Euler equations in hybrid coordinates (isopycnic + non-isopycnic) (thermodynamic coupling of density and pressure, Coriolis and wind-forcing)	2400 km × 1200 km	5 years	Formation and evolution of ocean gyres

Blumberg and Mellor (1987)	POM	RANS in σ-coordinates (hydrostatic, Coriolis forcing, Boussinesq approximation, equation of state, MY turbulence closure)	65 km × 700 km	2.5 days	Coastal trapped waves, upwelling, Ekman transport
Chen *et al.* (2003)	FVCOM	3D RANS equations in σ-coordinates (MY level 2.5 and Smagorinsky schemes for vertical and horizontal turbulence closures respectively)	Bohai sea (450 km × 500 km × 20 m)	10 days	Tidal amplitudes, residual currents and temperature variation
			Satilla river (40 km × 30 km × 4 m)	--	Tidal amplitudes, currents and residual currents
Shchepetkin and McWilliams (2005)	ROMS	Coupled barotropic (depth-averaged) and baroclinic (residual) momentum equations in hybrid $z-\sigma$ topography-following coordinates	--	--	--
Barron *et al.* (2006)	NCOM	RANS in surface-topography-following hybrid $\sigma - z$ coordinates (hydrostatic, Coriolis, Boussinesq, equation of state, MY turbulence closure, curvilinear surface mesh)	Global	~6 years	Sea-surface and depthward temperature variations
Chassignet *et al.* (2007)	HYCOM	Euler equations in hybrid coordinates (isopycnal + hydrostatic + σ) Open ocean to mixed-layer to coastal regions	Denmark Strait	--	Undersea overflow
			Gulf of Cadiz	--	Undersea overflow
			Gulf of Mexico	--	Sea surface height in the Gulf Stream
				--	Chlorophyll concentration in the Gulf Stream
			North Atlantic	--	Sea-surface temperature
				--	Salinity and temperature gradients
Barth *et al.* (2008)	ROMS + HYCOM	RANS equations in topography-following coordinates + Euler equation in hybrid coordinates (ROMS fully nested in HYCOM)	West Florida Shelf	~1 year	Effect of deep-ocean currents on shelf circulation
Haidvogel *et al.* (2008)	ROMS	RANS equations in topography-following coordinates (Hydrostatic, Boussinesq approximation, $k-\epsilon$ and $k-\omega$ turbulence closures, Ecological sub-routines, Rheology and Thermodynamics for sea-ice)	Hudson river estuary	50 days	Tidal dynamics, salt transport
			NENA continental shelf	3 years	Nitrogen cycling
			North Pacific Basin	6 years	Basin-scale climate modelling
			Barents Sea	12 years	Sea-ice distribution and dynamics
Bomminayuni *et al.* (2012)	FVCOM	3D RANS equations in σ-coordinates (MY level 2.5 and Smagorinsky	Rose Dhu Island (40 km ×	32 days	Identification of hydrokinetic energy hotspots

		schemes for vertical and horizontal turbulence closures respectively)	40 km)		from tidal streams
Delandmeter *et al.* (2018)	SLIM 3D	3D Hydrostatic Boussinesq equations in ALE formulation (Equation of state to correlate density, temperature and salinity, Coriolis forcing, Smagorinsky and $k-\epsilon$ closures for horizontal and vertical turbulence respectively)	Lake Tanganyika (650 km × 50 km × 0.57 km)	~3 years	Dynamics of thermocline oscillations in a lake
Adcroft *et al.* (2019)	MOM6 + OM4	3D Hydrostatic Boussinesq equations in generalized orthogonal curvilinear coordinates with vertical Lagrangian remap (Equation of state to correlate density, temperature and salinity; Coriolis forcing; EPBL for planetary boundary layer; MLE for baroclinic eddies; parameterizations for shear instabilities, internal breaking waves, BBL, lateral friction and mesoscale eddies; SIS2.0 model for sea-ice and icebergs)	World Ocean	300 years	Ocean-surface climate in terms of sea-surface temperature Seasonal cycling of mixed layer depths (MLDs) Ocean ventilation Temperature and currents in the upper ocean Arctic and Antarctic sea-ice
Hanert *et al.* (2023)	SLIM 2D	Nonlinear SWE (Horizontal baroclinity, surface wind-stress, turbulent diffusion, bottom-drag)	Persian / Arabian Gulf (gulf-scale to coastal-structures-scale)	~1 month	Multi-scale regional circulation patterns

Referring to Table 6, the popular ocean models include POM, FVCOM, ROMS, HYCOM and MOM6. The horizontal variable arrangement in these models is based on various classes of the finite-difference Arakawa grids, namely:

- **A-grid** in which scalars (eg. temperature and salinity) and vectors (eg. velocity) are defined at the same point,
- **B-grid** in which scalars are staggered from the velocity by half a grid dimension, however both velocity components are defined at the same point and
- **C-grid** in which both velocity components as well as scalars are staggered by half a grid dimension from one another.

In the vertical direction, the following coordinate system(s) are implemented:

- z-coordinates which follow the vertical direction and are suitable for resolving free-surface flow features,
- σ-coordinates which follow the bottom topography/bathymetry and are suitable for resolving the bottom boundary layer and
- isopycnal or isopycnic coordinates which follow the density contours and are suitable for resolving tracer (temperature, salinity etc.) transport in the open ocean.

As evidenced from Table 6, most ocean models employ some combination of the above coordinates which accords the capability for multi-scale simulations. A hybridization of coordinates is necessary because free-surface features, topographical features and density stratification all occur at different vertical scales and moreover the individual scales vary as one move from the open ocean to coastal regions (Chassignet *et al.*, 2007). Another important aspect which differentiates OGCMs from FNPT and BSNQE approached is the need for modelling the feedback from the subgrid-scales to the inertial-scales in terms of both momentum as well as scalar transport (turbulent diffusion). Referring to Table 6, this is achieved through various turbulence closure models. It is also interesting to note that, because the horizontal scale in such problems is significantly greater than the vertical scale (cf. select domain sizes in Table 6), the horizontal and vertical directions employ different turbulence closures. Typically, the Smagorinsky model (zero-equation turbulence model wherein the evaluation of μ_t is conceptually similar to Prandtl's mixing length model (Rodi *et al.*, 2013)) can be applied in the horizontal direction whilst a more comprehensive two-equation model (the MY-2.5 model is a popular choice; cf. Mellor and Yamada (1982) and Chen *et al.*, (2003) for details) can be applied in the vertical direction. This unique numerical constitution makes ocean models ideally suited for multi-scale modelling across a wide range of applications which is evidenced from Table 6. It is worth mentioning that the present review only aims at providing a brief overview of the development of OGCMs for the sake of completeness in context to multi-scale modelling and is by no means comprehensive. The reader should refer to the literature listed in Table 6 for further details.

6 Coupled models

In the previous sections, we presented several different models that are available to treat the problem at hand. However, rather than different models, it would be ideal to have one particular model to handle a wide range of problems spanning various spatio-temporal scales. One way of achieving this, as discussed in context to ocean sciences in §5, is to employ hybrid coordinate systems. Another way of achieving this is coupling different modelling tools that are developed over the period of years leading to multi-scale modelling in ocean engineering. Such coupled models are discussed in the following subsections.

6.1 Overview of coupling/decomposition strategies

With regards to coupling models, there are two approaches; one is domain decomposition and the other functional decomposition. The domain decomposition (DD) strategy divides the computational domain into parts and applies different mathematical models in each part. This is ideally done to avoid computationally expensive (and energy dissipative) NS simulations in the entire domain. Thus, multi-scale modelling is achieved by gaining the ability to model larger computational domains than would normally be allowed for a pure NS model. The functional decomposition (FD) strategy was pioneered by Dommermuth (1993) who simulated the formation of striations and scars on a free-surface due to impingement by a pair of vortex tubes shed from the tips of a submerged delta wing. In the case of FD, rather than physically decomposing the domain, the instantaneous velocity and pressure fields are decomposed into irrotational and vortical components. Another key characteristic of FD is the prescription of a constraint that the normal component of the vortical velocity is zero at the free-surface. This yields a transport equation for the free-surface elevation η in terms η and the velocity potential ϕ which accords an FNPT-like framework for the solution of

$\eta(x, y, t)$. Such a numerical treatment means that FD yields “natural and exact transition” from viscous vortical flow to inviscid vortical flow to potential flow (Dommermuth, 1993); this is not possible in a conventional primitive-variable formulation of the NSE.

6.2 Navier-Stokes coupled with potential-flow models (Domain Decomposition)

In most DD-based problems, the computational domain is decomposed into a viscous inner sub-domain and a potential outer sub-domain. The information (velocity, pressure and surface elevation) will be transferred through either relaxation zones or a sharp interface. Also, based on how the information between the solvers is being transferred, it can be either one-way coupling (weak coupling) or two-way coupling (strong coupling). In one way coupling, information is transferred only from the potential solver into the viscous solver, but in two-way coupling, the information is transferred in both ways, from depth-averaged or depth-resolving irrotational models to full NS and vice-versa. The two-way coupling is advantageous since it allows for a significantly smaller computational region for the viscous solver. However, it necessitates an iterative process or an implicit approach between the two models on a shared interface, which might increase the computational costs (Sriram *et al.*, 2014). The advantage of one-way coupling is that no such iterations are needed, but it needs a longer viscous domain to avoid the reflection from outer boundaries. This method is suitable, wherein, one needs to analyse the kinematics of the breaking waves in deep water or depth-induced breaking in the shallow water region (Saincher and Sriram, 2023).

An early implementation of the concept of weakly-coupled hybrid modelling can be seen in the work of Fujima *et al.* (2002). They spatially nested a three-dimensional Navier-Stokes model within a two-dimensional nonlinear long-wave model to simulate tsunami-breakwater interaction at $1:200$ scale. An obvious shortcoming of the model was that spanwise vortices generated in the depth-resolving model that could not be transferred back to the depth-averaged model due to the latter’s reduced dimensionality. Grilli and co-workers (1999, 2003, 2004) coupled the 2D HOBEM-FNPT with NS model based on SL-VOF. Extension of the FEM code with the NS model has also been carried out by Clauss and co-workers (2004, 2005). For the NS model they have tested with the commercial softwares such as FLUENT, CFX and COMET. They tested their coupling approach by studying the deep water wave breaking (breaking of freak waves) and comparing with experimental measurements. Yan and Ma (2009) coupled the QALE-FEM with the commercial software STAR-CD to study the wind effects on breaking waves. Hildebrandt *et al.* (2013) coupled the FEM with the commercial software ANSYS to model the wave impacts with tripod structure. Narayanaswamy *et al.* (2010) and Kassiotis *et al.* (2011) used one way coupling of the Boussinesq model with the SPH method for solitary wave simulations. Without feedback from the SPH to the Boussinesq model, a fixed overlapping zone was considered to transfer the information. Recently, this was improved by Agarwal *et al.*, (2022b) by coupling a Boussinesq model with the MLPG (Meshless Local Petrov Galerkin) method.

However, if one needs to analyse the wave structure interactions in the presence of floating bodies or fixed structure, then strong coupling of the two models is required, wherein the radiated waves will propagate from NS model to depth-averaged or depth-resolved irrotational models. In strong coupling, the computational domain is divided into two parts, in one part the generation and propagation of waves is being considered and in the other part structure/breaking region will be present. The modelling of first part of the domain will be carried out using depth-averaged or depth-resolved irrotational models and then the boundary conditions (velocity and pressure) are fed into the NS model at the same time steps, to study the remaining part of the domain. Then the velocity from NS model is again feed back to the depth-averaged or depth-resolved irrotational model domain for the next time step. Thus, in general, the strong coupling needs to couple the models both in space and time domains. For the coupling in space domain, the following four methods have been found to be employed, as pointed out by Sriram *et al.* (2014): (a) fixed boundary interface, (b) moving boundary interface, (c) fixed overlapping zone and (d) moving overlapping zone.

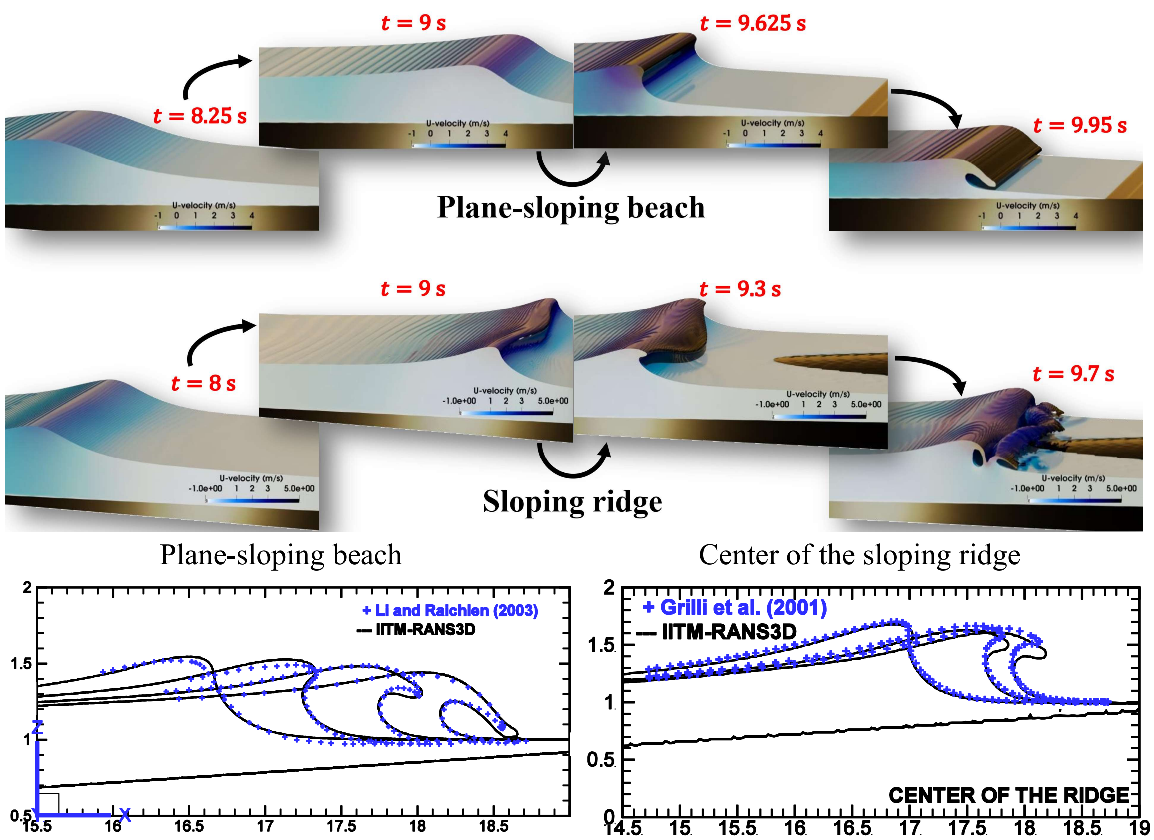

Figure 8. Simulation of solitary wave-breaking over a $1:15$ *plane-sloping beach and sloping ridge using weakly coupled IITM-FNPT2D and IITM-RANS3D: (top) topology of the over-turning wave visualized using iso-volumes of VOF and coloured using streamwise velocity, (bottom) validation of the breaking topology against literature (Saincher and Sriram, 2023).*

One of the pioneering works in this regard was carried out by Grilli and co-workers (2005, 2010) wherein, they extended the model from weak coupling to strong coupling for studying the 3D breaking waves by coupling 3D HOBEM-VOF. Later, Grilli and co-workers (2007, 2008, 2009) coupled the NWT and NS based on Large Eddy Simulation (LES) to study the forced sediment transport simulations. Later studies from Greco (2001), Colicchio *et al.* (2006), Greco *et al.* (2007) and Sitanggang and Lynett (2010) further established the feasibility of the DD strategy. Following these studies, a ground-breaking contribution was made by Sriram *et al.*, (2014) wherein the full capability of coupled DD modelling was explored in detail.

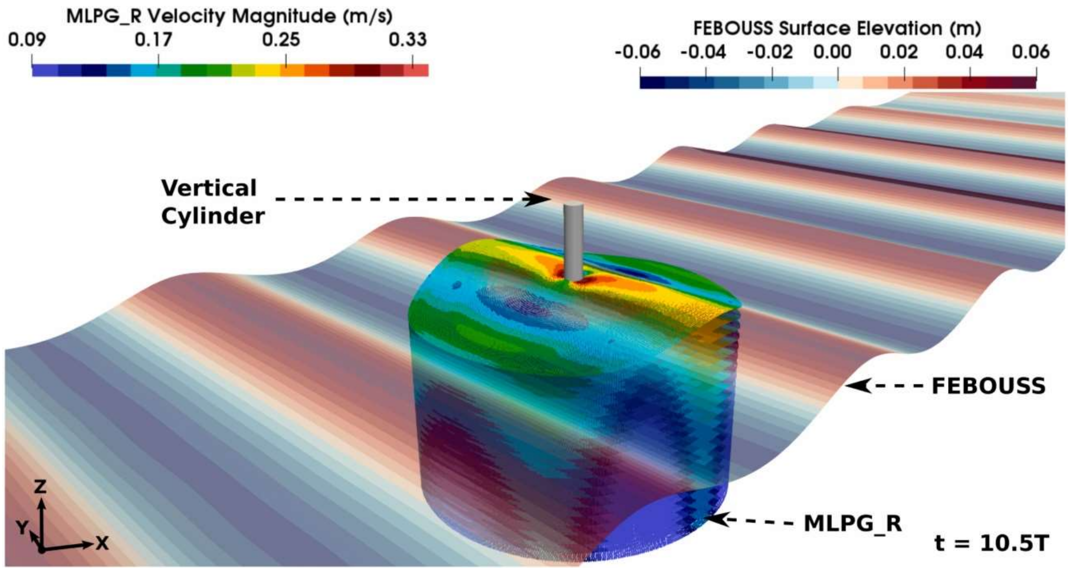

Figure 9. Simulation of directional regular waves (aligned at 30° *to the* x*-axis) interacting with a fixed cylinder using weakly coupled FEBOUSS and MLPG_R using 3D cylindrical coupling interfaces (Agarwal et al., 2022b).*

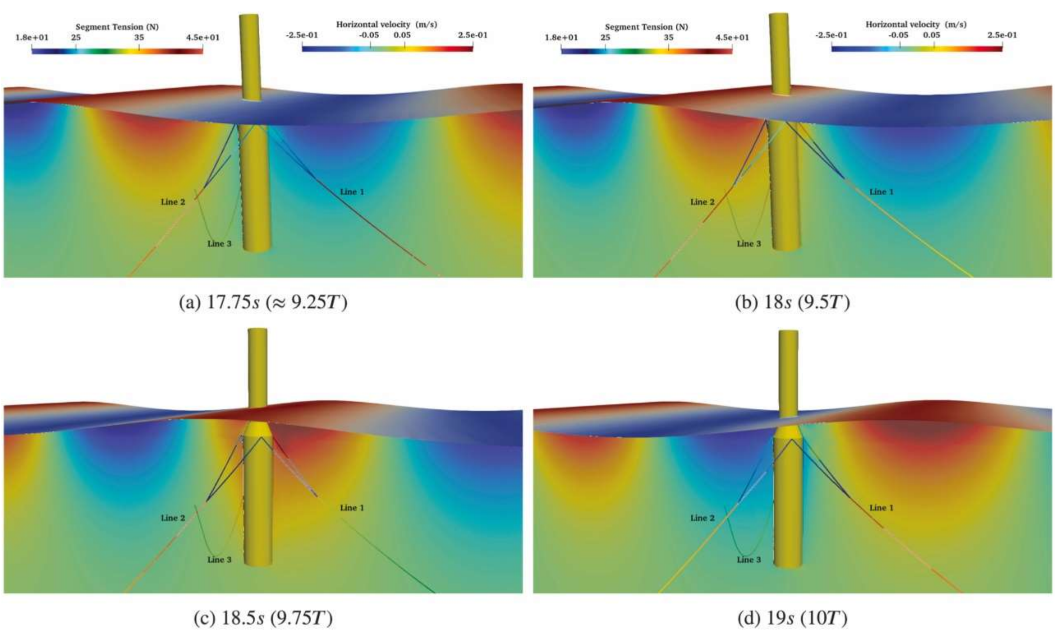

Figure 10. Simulation of regular waves interacting with a moored floating spar using a coupled model employing HOS-NWT, foamStar and MoorDyn (Aliyar et al., 2022).

However, until now mostly these strong coupling are realised only in the 2D problems, and, to the best of the authors' knowledge, the strong coupling in 3D is yet to be attempted. Typical examples of simulations performed based on one-way coupling using the codes developed by the authors and their co-workers: IITM-RANS3D, HOS-NWT-foamstar (using depth-resolved potential and viscous models) and FEBOUSS-MLPG (using depth-averaged potential and viscous models) are reported in Figures 8-10.

One more popular hybrid model is qaleFOAM, which has been developed based on the experience from QALE-FEM. This model adopts the domain decomposition approach, which combines a two-phase Navier–Stokes (NS) model with a model based on the fully nonlinear potential theory (FNPT). In a region around the structures and/or the breaking waves (NS domain), the open-source NS solver OpenFOAM/interDyMFoam is applied. In the rest of the computational domain (FNPT domain), the FNPT-based quasi arbitrary Lagrangian–Eulerian finite element method (QALE-FEM) is adopted. The qaleFOAM was originally developed for modelling the turbulent flow near offshore structures subjected to extreme waves (Li *et al.*, 2018). It has now been extended and applied to model a wide range of wave-structure interaction problems, such as the wave resistance (e.g. Gong *et al.*, 2020), violent wave impact on sea walls (Li *et al.*, 2023), survivability and performance of floating wind turbines (Yu *et al.*, 2023; Yuan *et al.*, 2023) and wave energy converters (Yan *et al.*, 2020) as well as wave-driven drift of floating objects (Xiao *et al.*, 2024). Recently blind tests and numerical comparative studies have confirmed its superiority over single-model methods including the potential theory and the NS solvers. The details will be discussed below. However, one of the theoretical issues in these DD coupling is that the researchers coupled irrotational flow model with the rotational flow models. Particularly for strong coupling, there is a mathematical discontinuity in the velocity field and they overcome this with numerical approaches (Sriram and Ma, 2021). This needs to be overcome in the future modelling efforts, see Yang and Liu (2022) for the development of the multi-layer model based on rotational flow.

6.3 Navier-Stokes coupled with potential-flow models (Functional Decomposition)

As described earlier in §6.1, the fundamental concept for the functional decomposition (FD) is to use the Helmholtz decomposition to separate the velocity field into the rotational and irrotational parts to investigate the free surface flow (Dommermuth, 1993). The FD approach has also been adopted to simulate ocean engineering scenarios. In context to WSI, there are two categories under this decomposition, based on whether the structure is considered in the potential solver or not.

6.3.1 First category: structure handled by both potential and viscous solvers

In the first category, the WSI problem is split into a potential component and a viscous part. The complete problem is initially solved by a potential solver, and then rectified by adding the viscous correction (Kim *et al.*, 2005; Edmund *et al.*, 2013; Rosemurgy *et al.*, 2016; Robaux and Benoit, 2021). One drawback of this strategy is that the potential solver must first solve the entire problem before applying the viscosity correction. As a result, challenges such as higher-order waves, stability issues in the steep waves and breaking induced by presence of structure with complex interactions are still constraints in this classification. Recently, Robaux (2020) published a thorough description of nonlinear waves' interactions with a horizontal cylinder with a rectangular cross section employing potential solver, CFD solver, and HPC-OpenFOAM coupled DD and FD based solvers. In comparison to the full CFD simulation, both coupling approaches, in particular the FD-based approach, need a minimal amount of computational time while providing an accurate representation of the loads and associated hydrodynamic coefficients.

6.3.2 Second category: structure only handled by the viscous solver

In the second category, the total unknown is decomposed into the incident part and the complementary part. Only the incident flow is modelled in the incident part (wave only), leaving all the interaction with structure calculated by the viscous solver as the complementary part. The common name among researchers for this classification is SWENSE (Spectral Wave Explicit Navier Stokes Equations), proposed by (Ferrant *et al.*, 2002) and actively developed by (Gentaz, 2004; Li *et al.*, 2018; Kim, 2021). The NS equation modified into the SWENSE is solved to yield the complementary fields. The advantage of this method is that the wave models directly provide incident wave solutions, minimising the problem's complexity and cost. For a detailed derivation of single-phase and two-phase SWENSE, refer to Luquet *et al.* (2007) and Li *et al.* (2018) respectively. The applications in single-phase SWENSE over the years can be read in (Luquet *et al.*, 2007; Monroy *et al.*, 2010). Recently, the two-phase SWENSE method (Li *et al.*, 2021) has been implemented on top of *foamStar* and is called as *foamStarSWENSE*, and the only difference is that in this solver, the NS equations in *foamStar* are replaced by SWENSE. Recent developments of *foamStarSWENSE* such as efficient regular and irregular wave generation in the solver and higher-order forces estimation on a vertical cylinder, buoy and floating spar can be referred to in Choi (2019), Kim (2021), Li *et al.* (2018) as well as in Aliyar *et al.* (2022).

6.4 Navier-Stokes coupled with geophysical fluid dynamics / ocean-science models

Recently, there has been a research effort to implement the domain decomposition (DD) strategy to (strongly) couple geophysical fluid dynamics (GFD) / ocean-sciences models with Navier-Stokes solvers. A couple of such hybrid GFD-CFD models have been listed in Table 7 wherein FVCOM (cf. Table 6 for details) has been coupled to either the overset mesh-based single-phase NS solver SIFOM or the unstructured mesh-based two-phase NS solver SIFUM. It is worth mentioning that in addition to the NS solver being based on overset meshes (SIFOM), the overset grids have also been employed to nest the SIFOM/SIFUM domain within the FVCOM domain. Referring to the domain sizes in Table 7, it should be noted that in some cases, the SIFUM domain is not necessarily entirely nested within the FVCOM domain along the vertical (z) direction. This is attributable to the ability to model the air-phase within the SIFUM framework which is necessary for violent WSI scenarios.

Such hybrid GFD-CFD modelling provides the ability to perform multi-scale environmental, geological as well as FSI/WSI simulations over domains spanning several hundred or even several thousands of square kilometres. However, it is worth mentioning that some of the problems listed in Table 7 are comparatively "small-scale" and can indeed be tackled by more conventional FNPT-RANS models. For instance, Saincher and Sriram (2022b) have applied IITM-RANS3D to a $0.045 \times 0.0022 \times 0.002\ \mathrm{km}^3$ domain to simulate the interaction between focusing waves and a moving cylinder. In another study Saincher et al. (2021) had applied IITM-RANS3D to a $0.3 \times 0.005 \times 0.007\ \mathrm{km}^3$ domain to study the run-up characteristics of violently breaking long and high waves that could be generated by an extreme coastal event. Thus, the lower-limit of applicability of the hybrid GFD-CFD models can also be tackled by hybrid FNPT-RANS models.

Table 7. A brief overview of geophysical fluid dynamics / ocean science models recently hybridized with Navier-Stokes equations models reported in the literature; cf. nomenclature for abbreviations. (✘: data unavailable)

Authors	**Models**		**Maximum domain extents for each model**		**Coupling strategy**	**Application**
	Large-scale	**Small-scale**	**Large (km³) $(x \times y \times z)$**	**Small (km³) $(x \times y \times z)$**		
Tang *et al.* (2014)	FVCOM (weakly 3D)	SIFOM (fully 3D, single-phase)	$1.8 \times 0.6 \times 0.1$	$0.4 \times 0.4 \times 0.1$	DD (strong coupling)	Flow over flat plate
			$3.5 \times 0.4 \times 0.15$	$\sim 2.0 \times 0.3 \times 0.1$		Transient sill flow
			$3 \times 0.3 \times 0.009$	$\sim 0.05 \times 0.02 \times 0.009$		Bridge pier (lab-scale)
			$3 \times 0.6 \times$ ✘	$\sim 0.8 \times 0.4 \times$ ✘		Thermal effluent
			$\sim 70 \times 140 \times 0.013$	✘		Bridge pier (river-scale)
			$\sim 170 \times 170 \times 0.05$	$\sim 0.7 \times 0.7 \times 0.05$		Flow past seamount
Qu *et al.* (2016)	FVCOM (weakly 3D)	SIFOM (fully 3D, single-phase)	$3 \times 0.6 \times 0.012$	$0.075 \times 0.03 \times 0.012$	DD (strong coupling)	Thermal effluent
			$\sim 20 \times 15 \times 0.004$	✘		Lagrangian tracking of estuary flows
			$\sim 250 \times 1 \times 0.01$	✘		Storm surge impact on river bridge pier
Qu *et al.* (2019a)	FVCOM (weakly 3D)	SIFUM (fully 3D, two-phase)	$14 \times 0.1 \times 0.2$	$\sim 2 \times 0.1 \times 0.05$	DD (strong coupling)	Tsunami wave runup
						Tsunami wave impacting coastal highway bridge
Qu et al. (2019b)	FVCOM (weakly 3D)	SIFUM (fully 3D, two-phase)	$3.5 \times 0.4 \times 0.15$	$\sim 1 \times 0.3 \times 0.225$	DD (strong coupling)	Transient sill flow
			$0.2 \times 0.2 \times 0.01$	$\sim 0.1 \times 0.12 \times 0.01$		3D dam-break flow
			$0.04 \times 0.001 \times 0.0004$	$0.004 \times 0.001 \times 0.0005$		Long-wave impingement on a vertical cylinder
			$0.04 \times 0.03 \times 0.002$	$0.015 \times 0.03 \times 0.002$		Hydraulic jump
			$\sim 60 \times 60 \times 0.025$	$\sim 0.1 \times 0.1 \times$ ✘		Coastal flood impacting beachfront house

7 Benchmarking the Numerical Models through Comparative Studies

In the past researchers developed numerical models and validated with their own experimental simulations, the data sharing and comparison between different numerical models, its accuracy and performance in terms of computational efficiency are not attempted. In the field of ocean engineering, when the concept of numerical wave tank was developed inline with the numerical wind tunnels that are quite popular in those times, Clément (1999) and Tanizawa and Clément (2000) carried out such exercise for fully nonlinear potential flow theory. Recently, major initiatives were undertaken by Ransley *et al.* (2019, 2020), Sriram *et al.* (2021), Agarwal *et al.* (2021a) and Saincher *et al.* (2023a). These studies highlighted some of the commonly adopted guidelines by the researchers pertaining to WSI simulations:

- The fidelity of regular/focusing wave generation deteriorates away from the wavemaker irrespective of the nature of the numerical model and no single wave-generation method may be regarded as superior over others. Far from the wavemaker, the models generally deviate by $5-10\%$ in terms of primary energy content which is acceptable. However, the deviation across models may be as high as 50% in terms of the sub- and super-harmonic wave components.

- The performance of a solver should be judged based on the peak values of the surface-elevation/hydrodynamic pressures/loads as well as the phase agreement captured by the model. Phase disagreement is acceptable for WSI scenarios involving regular waves (Saincher et al., 2023a) as long as the phase-shift remains constant over several wave cycles. However, for WSI scenarios involving transient waves such as focused and/or overturning waves, the phase agreement is critical as it determines the shape of the impacting wave as well as the time-varying load profile on the structure (Sriram *et al.*, 2021 ; Agrawal *et al.*, 2021a).
- The inclusion of turbulence modeling does not necessarily improve the accuracy of a simulation. This rather depends on the problem at hand. Further, for the same problem, different turbulence models may lead to the same/similar results. The expertise of the user should also be factored-in whilst using turbulence models, especially RANS-based models which are strongly empirical. These statements are substantiated through Figure 11 wherein results from the ISOPE-2022 comparative study on WSI are reported. In this study, one of the participating institutions had employed STAR-CCM+ for the simulations and had assessed the effect of different turbulence modeling strategies (implicit LES ("laminar"), RANS and explicit LES) on the solution. It can be observed from Figure 11 that changing the modeling strategy hardly affects the pressure time-history or the value of maximum impact pressure across multiple loading cycles. This could be interpreted from two perspectives: (a) the physics of the problem under consideration is independent of turbulence modeling or (b) the employed numerical framework is independent of turbulence modeling. The first statement is (obviously) incorrect. The second interpretation, however, holds merit from the standpoint of the relation between LES and RANS (Rodi *et al.*, 2013). It is worth mentioning that the STAR-CCM+ simulations were two-dimensional and a rather coarse resolution of $L/300$ and $H/50$ (where L is the wavelength and H is the wave-height) was chosen for the horizontal and vertical directions respectively. This corresponds to a mesh-size of $\Delta x \sim 12$ cm and $\Delta z = 1.4$ cm respectively which is comparable to the $\Delta x = \Delta z = 5$ cm chosen for the RANS model IITM-RANS3D in the same study (Saincher *et al.*, 2023a). The numerical framework exhibits "independence" from turbulence modeling because a RANS resolution was applied to LES and ILES. Since the transport equations for the mean-flow are the same between unsteady RANS and LES (Rodi *et al.*, 2013), STAR-CCM+ apparently resolved the same mean-flow in all three cases. The minor differences in peak impact pressure observed in Figure 11 stem from the unresolved scales that are modeled differently across RANS, ILES and LES (Rodi *et al.*, 2013).

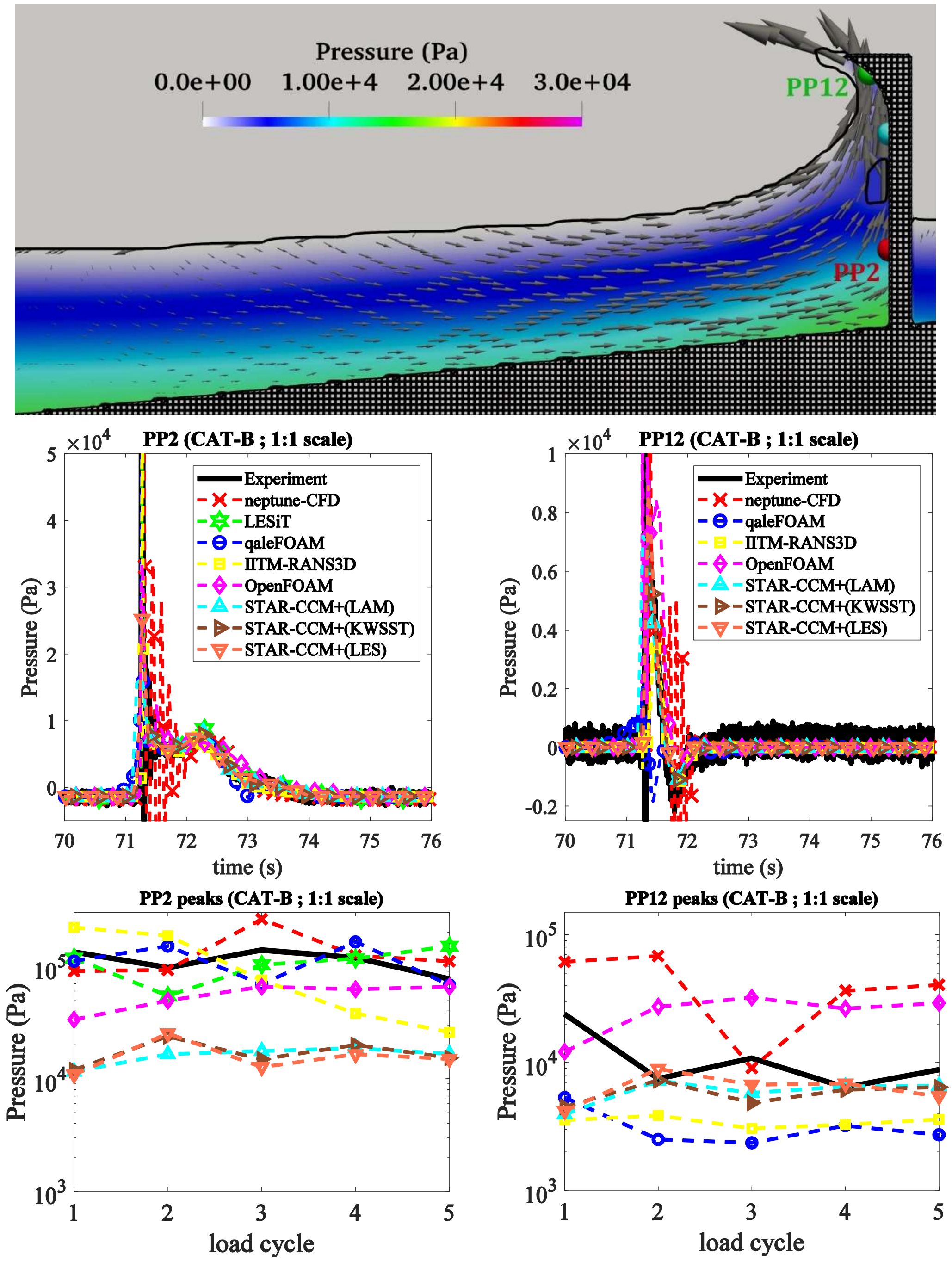

Figure 11. Results from the ISOPE-2022 comparative study on breaking waves impacting a seawall with a recurved parapet (Saincher et al., 2023a): (top) seaward deflection of the breaking wave, (center) time-history of the hydrodynamic pressure over the vertical wall (PP2) as well as the parapet (PP12) and (bottom) variation of peak impact pressure over five loading cycles.

It is also worth noting that had the opposite been done wherein an LES grid was applied to RANS, dramatically different results would have been obtained. This is because RANS would have become grid-independent on the scale of the LES grid whilst LES itself would only become grid-independent at the Kolmogorov scale (Rodi *et al.*, 2013). Thus, one might argue that this instance constitutes a case where turbulence modeling was attempted but eventually proved to be unnecessary.

- Hybrid modeling invariably improves the computational efficiency of the solver and should be adopted for large-scale WSI problems (Agarwal *et al.*, 2021a ; Saincher *et al.*, 2023a).
- The state of the art in modelling large domain problems for transient waves appeared to be based on hybrid numerical modelling using weakly coupled algorithms (or one-way coupling); this strategy was adopted by most of the participants.
- In simulating the same WSI problem at different scales, no general correlation could be obtained between computational effort and the scale of the problem. For instance, amongst the ten models compared for breaking waves interacting with a recurved seawall, the hybrid codes qaleFOAM and IITM-RANS3D were simultaneously the fastest and slowest at two different scales of the problem (Saincher *et al.*, 2023a).

In these studies it was also noted that the experimental error/uncertainty should be taken into consideration during validation. The inclusion of the experimental uncertainty would make the above guidelines less stringent. However, a conservative approach is beneficial in order to maintain a reduced error margin when adopting the said guidelines in practice.

8 The Future

8.1 Application of machine learning algorithms

The machine learning (ML) techniques is becoming popular in assisting the fluid simulation, e.g. to reconstruct the fluid field from data (Raissi *et al.*, 2020), to predict the turbulence related parameters (Ling *et al.*, 2016; Zhang *et al.*, 2015; Kutz, 2017), and to approximate time-independent flow filed governed by NS models, such as the projection-based Pressure Possion Equation (PPE, e.g. Yang *et al.*, 2016; Xiao *et al.*, 2018; Tompson *et al.*, 2017; Dong *et al.*, 2019; Ladicky *et al.*, 2015; Wessels *et al.*, 2020, Li *et al.*, 2022). Recently, both the convolution neural network (CNN, Zhang *et al.*, 2023) and graphic neural network (GNN, Zhang *et al.*, 2024a, 2024b) have been coupled with the incompressible smoothed particle hydrodynamics (ISPH) model to accelerate the numerical simulations. In these work, high-fidelity time-domain numerical results are produced using stand-alone ISPH simulation on wave propagation and impact on fixed structure. The CNN or GNN are used to train a machine learning algorithm to predict the pressure in the future step based on the numerical results at the current time step including the velocity, velocity divergence and pressure. After the algorithm is trained, it will be used to replace the PPE solver in the classic ISPH. Both the CNN-supported and GNN-supported ISPH models have been applied to modelling wave propagation, impact on seawall and interaction with other structures. Figure 12 and Figure 13 illustrate some numerical results from the GNN-supported ISPH, which does not only show the capacity of the ML-supported ISPH but also demonstrate its promising accuracy. Further evidence on numerical accuracy and CPU speeding-up can be demonstrated in Figure 14 for the cases with solitary wave propagation. In this figure, the error is defined by the L2-norm of the time history of the wave crest; ISPH and ISPH-CQ adopt the linear and 2^{nd}-order PPE solvers, respectively.

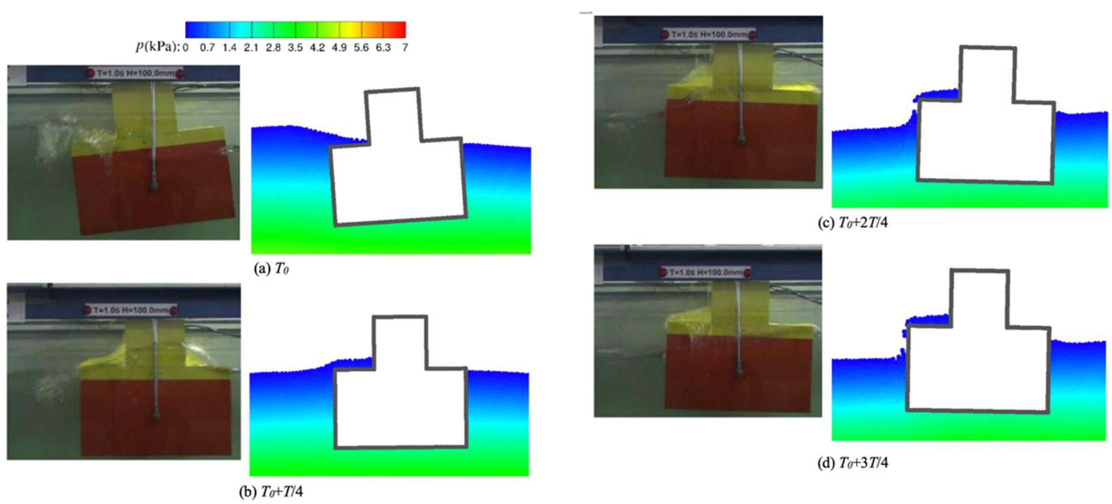

Figure 12. Comparisons of the floater movement progress during green water impact between laboratory photos (Zheng et al., 2016) (left) and ISPH_GNN simulations (right) at different instants (duplicated from Zhang et al., 2024b).

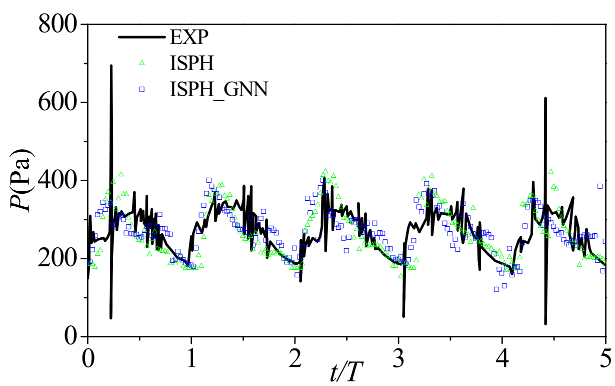

Figure 13. Time histories of the impact pressure on deck at P1 (duplicated from Zhang et al., 2024b).

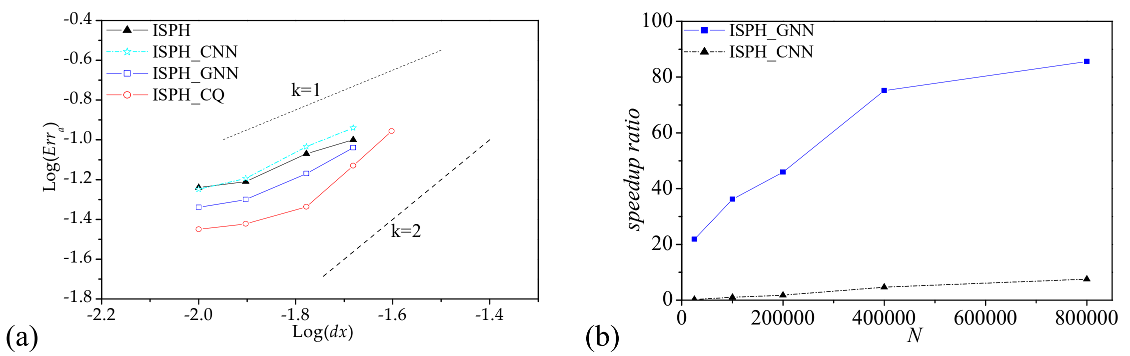

*Figure 14. Averaged errors of numerical results corresponding to different particle spacing in the solitary wave propagation (a) and the CPU speeding ratio (b) against solving PPE directly (solitary wave height = 0.28*water depth ; duplicated from Zhang et al., 2024a).*

As shown in Figure 14(a), both the convergence and accuracy of the ISPH-GNN are bounded by the corresponding values of the ISPH and ISPH-CQ, implying a promising computational accuracy. Figure 14(b) illustrates excellent CPU time speeding-up ratios against directly solving the PPE using the 2nd order solver. For the solitary wave propagation using 80k particles, the GNN can speed up the simulation by 80 times.

The existing work related to AI and ML may be quantified as hybrid model combing a CFD solver with the ML algorithms, e.g. Zhang *et al.* (2024a) combining ISPH with graph neural network for simulating free surface flows. Data are needed to train the ML algorithms. Recently, researchers started solving the fluid mechanics and fluid-structure interaction problems using the AI library for discretising the required partial differential equation (AI4PDE, see, e.g. Chen *et al.*, 2024). This work does not need to train the neural network but directly modifying the filters of the neural network. Limited benchmarking rest has demonstrated its promising computational accuracy and efficiency. The applications of the AL/ML to existing hybrid model, such as the qaleFOAM, have yet found to the best of our knowledge. Based on our preliminary work on CNN/GNN supported ISPH, its feasibility to the hybrid modelling is confirmed.

The challenges in the hybrid modelling can be fully or partially solved by the AL/ML technologies. These include: (1) replacing the NS solver by the ML-supported version; (2) intelligently decomposing the computational domain in an adaptive way, i.e. to minimising the NS domain in the run-time depends on the development of the viscosity/turbulence effect and breaking wave occurrence; (3) intelligently choosing the appropriate models, such as RANS or LES; (4) in the function-decomposition approach, using the ML algorithms for solving the compromised equations instead of solving them directly; (5) dynamic load balancing in the cases with parallel computing.

8.2 Hybrid FNPT-RANS-LES models for floating renewables

Another important aspect in the blue economy theme is the renewable energy. The development of offshore wind farms based on Floating Offshore Wind Turbine (FOWT) arrays is one of the popular, potential and realizable area. In order to reduce the CAPEX and installation costs, shared mooring systems have been proposed for FOWT arrays where anchors and a part of the mooring line are shared between turbines. This introduces challenges that manifest differently in shallow and deep water. The deep-water mooring system is susceptible to motions of the FOWT platform being amplified leading to large displacements in the mooring line and peak anchor loads. Chain catenary moorings in shallow water experience snap loads due to their susceptibility to violent wave-current-structure interactions during extreme events and individual loads superimposing nonlinearly with the structural response. In order to develop a comprehensive understanding of the mechanisms leading to snap loads and peak anchor forces in shared mooring systems of a FOWT farm, high fidelity multi-scale solver is required. To achieve this, the existing FNPT (Fully Nonlinear Potential Theory), RANS (Reynolds Averaged Navier-Stokes) and Large Eddy Simulation (LES) codes can be coupled via a zonal approach to yield a high-fidelity multi-scale solver for wave-current-structure interaction. A FEM-based structural solver will be integrated to accurately predict the coupled fluid-structure interaction of several mooring lines and to facilitate the modelling of elastic materials. A critical aspect of the model development would be scaling-up the code for prototype-scale FOWT arrays whilst retaining computational efficiency and accuracy. This could be achieved using AI and ML-based prediction of turbulence-generation near the floating platforms, as this is expected to be the most computationally intensive aspect of the modelling (traditionally handled using hybrid RANS-LES). Thus, a continuous research efforts in the field of computational hydrodynamics is required. This is in fact supported by the Newton Fellowship (recently awarded to the second author from the authors research group in 2023) wherein the existing understanding in hybrid modelling as well as AI/ML-based prediction of turbulence shall be carried forward.

Acknowledgement

The first author acknowledges the Newton International Fellowship for supporting the development of the numerical model in his group. Through the alumni funds of Newton Fellowship, the research group students (Dr. Rijas, Dr. Shagun Agarwal, Dr. Ravindar, Dr. Manoj Kumar, Mrs. Divya R, Dr. Shaswat Saincher) visited and benefited from the collaboration with UK universities. This work is partially supported by Center for Maritime Experiments to Maritime Experience (ME2ME), IIT Madras.

References

Adcroft, A., Anderson, W., Balaji, V., Blanton, C., Bushuk, M., Dufour, C. O., Dunne, J. P., Griffies, S. M., Hallberg, R., Harrison, M. J., Held, I. M., Jansen, M. F., John, J. G., Krasting, J. P., Langenhorst, A. R., Legg, S., Liang, Z., McHugh, C., Radhakrishnan, A., Reichl, B. G., Rosati, T., Samuels, B. L., Shao, A., Stouffer, R., Winton, M., Wittenberg, A. T., Xiang, B., Zadeh, N., & Zhang, R. (2019). The GFDL Global Ocean and Sea Ice Model OM4.0: Model Description and Simulation Features. *Journal of Advances in Modeling Earth Systems*, *11*, 3167-3211. https://doi.org/10.1029/2019MS001726

Agarwal, S., Saincher, S., Sriram, V., Yan, S., Xie, Z., Schlurmann, T., Ma, Q., . . . Ferrant, P. (2021a). A comparative study on the nonlinear interaction between a focusing wave and cylinder using state-of-the-art solvers: Part B. *International Journal of Offshore and Polar Engineering*, *31*(1), 11–18. https://doi.org/10.17736/ijope.2021.jc832

Agarwal, S., Sriram, V., Yan, S., & Murali, K. (2021b). Improvements in MLPG formulation for 3D wave interaction with fixed structures. *Computers & Fluids*, *218*, 104826. https://doi.org/10.1016/j.compfluid.2020.104826

Agarwal, S., Sriram, V., Liu, P., & Murali, K. (2022a). Waves in waterways generated by moving pressure field in Boussinesq equations using unstructured finite element model. *Ocean Engineering*, *262*, 112202. https://doi.org/10.1016/j.oceaneng.2022.112202

Agarwal, S., Sriram, V., & Murali, K. (2022b). Three-dimensional coupling between Boussinesq (FEM) and Navier–Stokes (particle based) models for wave structure interaction. *Ocean Engineering*, *263*, 112426. https://doi.org/10.1016/j.oceaneng.2022.112426

Aliyar, S., Ducrozet, G., Bouscasse, B., Bonnefoy, F., Sriram, V., & Ferrant, P. (2022). Numerical coupling strategy using HOS-OpenFOAM-MoorDyn for OC3 Hywind SPAR type platform. *Ocean Engineering*, *263*, 112206. https://doi.org/10.1016/j.oceaneng.2022.112206

Anbarsooz, M., Passandideh-Fard, M., & Moghiman, M. (2013). Fully nonlinear viscous wave generation in numerical wave tanks. *Ocean Engineering*, *59*, 73–85. https://doi.org/10.1016/j.oceaneng.2012.11.011

Anghan, C., Dave, S., Saincher, S., & Banerjee, J. (2019). Direct numerical simulation of transitional and turbulent round jets: Evolution of vortical structures and turbulence budget. *Physics of Fluids*, *31*(6). https://doi.org/10.1063/1.5095589

Anghan, C., Bade, M., & Banerjee, J. (2021). A modified switching technique for advection and capturing of surfaces. *Applied Mathematical Modelling*, *92*, 349–379. https://doi.org/10.1016/j.apm.2020.10.038

Anghan, C., Bade, M., & Banerjee, J. (2022). Direct numerical simulation of turbulent round jet released in regular waves. *Applied Ocean Research*, *125*, 103248. https://doi.org/10.1016/j.apor.2022.103248

Arote, A., Bade, M., & Banerjee, J. (2021). An improved compressive volume of fluid scheme for capturing sharp interfaces using hybridization. *Numerical Heat Transfer, Part B: Fundamentals*, *79*(1), 29–53. https://doi.org/10.1080/10407790.2020.1793543

Barron, C. N., Kara, A. B., Martin, P. J., Rhodes, R. C., & Smedstad, L. F. (2006). Formulation, implementation and examination of vertical coordinate choices in the Global Navy Coastal Ocean Model (NCOM). *Ocean Modelling*, *11*, 347-375. https://doi.org/10.1016/j.ocemod.2005.01.004

Barth, A., Alvera-Azcárate, A. & Weisberg, R. H. (2008). Benefit of nesting a regional model into a large-scale ocean model instead of climatology. Application to the West Florida Shelf. *Continental Shelf Research*, *28*, 561-573. https://doi.org/10.1016/j.csr.2007.11.004

Barthélémy, X., Banner, M. L., Peirson, W. L., Fedele, F., Allis, M., & Dias, F. (2018). On a unified breaking onset threshold for gravity waves in deep and intermediate depth water. *Journal of Fluid Mechanics*, *841*, 463–488. https://doi.org/10.1017/jfm.2018.93

Benoît, M., Benguigui, W., Teles, M. J., Robaux, F., & Peyrard, C. (2023). Two-phase CFD Simulation of Breaking Waves Impacting a Coastal Vertical Wall with a Recurved Parapet. *International Journal of Offshore and Polar Engineering*, *33*(2), 123–131. https://doi.org/10.17736/ijope.2023.sv03

Beji, S., & Nadaoka, K. (1996). A formal derivation and numerical modelling of the improved Boussinesq equations for varying depth. *Ocean Engineering*, *23*(8), 691-704. https://doi.org/10.1016/0029-8018(96)84408-8

Bihs, H., Kamath, A., Chella, M. A., Aggarwal, A., & Arntsen, Ø. A. (2016). A new level set numerical wave tank with improved density interpolation for complex wave hydrodynamics. *Computers & Fluids*, *140*, 191–208. https://doi.org/10.1016/j.compfluid.2016.09.012

Bleck, R. & Boudra, D. B. (1981). Initial Testing of a Numerical Ocean Circulation Model Using a Hybrid (Quasi-Isopycnic) Vertical Coordinate. *Journal of Physical Oceanography*, *11*(6), 755-770. https://doi.org/10.1175/1520-0485(1981)011%3C0755:ITOANO%3E2.0.CO;2

Blumberg, A. F., & Mellor, G. L. (1987). A Description of a Three-Dimensional Coastal Ocean Circulation Model. In N. S. Heaps (Eds.), Three-Dimensional Coastal Ocean Models (pp. 1–16). chapter, American Geophysical Union. https://doi.org/10.1029/CO004p0001

Bomminayuni, S., Bruder, B., Stoesser, T., & Haas, K. (2012). Assessment of hydrokinetic energy near Rose Dhu Island, Georgia. *Journal of Renewable and Sustainable Energy*, *4*(6), 063107. https://doi.org/10.1063/1.4766884

Brocchini, M. (2013). A reasoned overview on Boussinesq-type models: the interplay between physics, mathematics and numerics. *Proceedings of the Royal Society A: Mathematical, Physical and Engineering Sciences*, *469*(2160), 20130496. https://doi.org/10.1098/rspa.2013.0496

Bryan, K. (1969). A numerical method for the study of the circulation of the world ocean. *Journal of Computational Physics*, *4*(3), 347-376. https://doi.org/10.1016/0021-9991(69)90004-7

Bussmann, M., Kothe, D. B., & Sicilian, J. (2002). Modeling High Density Ratio Incompressible Interfacial Flows. *ASME 2002 Joint U.S.-European Fluids Engineering Division Conference*. https://doi.org/10.1115/fedsm2002-31125

Chassignet, E. P., Hurlburt, H. E., Smedstad, O. M., Halliwell, G. R., Hogan, P. J., Wallcraft, A. J., Baraille, R. & Bleck, R. (2007). The HYCOM (HYbrid Coordinate Ocean Model) data assimilative system. *Journal of Marine Systems*, *65*, 60-83. https://doi.org/10.1016/j.jmarsys.2005.09.016

Chen, B., Heaney, C. E., Gomes, J. L. M. A., Matar, O., & Pain, C. C. (2024). Solving the Discretised Multiphase Flow Equations with Interface Capturing on Structured Grids Using Machine Learning Libraries. *arXiv (Cornell University)*. https://doi.org/10.48550/arxiv.2401.06755

Chen, C., Liu, H., & Beardsley, R. C. (2003). An Unstructured Grid, Finite-Volume, Three-Dimensional, Primitive Equations Ocean Model: Application to Coastal Ocean and Estuaries. *Journal of Atmospheric and Oceanic Technology*, *20*(1), 159-186. https://doi.org/10.1175/1520-0426(2003)020%3C0159:AUGFVT%3E2.0.CO;2

Choi, Y. (2019). Two-way coupling between potential and viscous flows for a marine application. Ph.D. thesis. École centrale de Nantes. https://hal.science/tel-02493305/

Choi, J., & Yoon, S. B. (2009). Numerical simulations using momentum source wave-maker applied to RANS equation model. *Coastal Engineering*, *56*(10), 1043–1060. https://doi.org/10.1016/j.coastaleng.2009.06.009

Chorin, A. J. (1967). A numerical method for solving incompressible viscous flow problems. *Journal of Computational Physics*, *2*(1), 12–26. https://doi.org/10.1016/0021-9991(67)90037-x

Clément, A. (1999). Benchmark test cases for numerical wave absorption : 1st Workshop of ISOPE Numerical Wave Tank group, Montréal, May 1998. *The Proceedings of the 9th International Offshore and Polar Engineering Conference*, *3*, 266–289. https://onepetro.org/ISOPEIOPEC/proceedings/ISOPE99/All-ISOPE99/ISOPE-I-99-268/24902

Clauss, G. F., J. Hennig, and C. Schmittner (2004). Modelling extreme wave sequences for the hydrodynamic analysis of ships and offshore structures. Proceedings of *9th Symposium on Practical Design of Ship and other Floating Structures*, Lübeck Travemünde, Germany, September 12-17, 1-9.

Clauss, G. F., Schmittner, C. E., & Stück, R. (2005). Numerical Wave Tank: Simulation of Extreme Waves for the Investigation of Structural Responses. *ASME 2005 24th International Conference on Offshore Mechanics and Arctic Engineering*. https://doi.org/10.1115/omae2005-67048

Colicchio, G., Greco, M., & Faltinsen, O. M. (2006). A BEM-level set domain-decomposition strategy for non-linear and fragmented interfacial flows. *International Journal for Numerical Methods in Engineering*, *67*(10), 1385–1419. https://doi.org/10.1002/nme.1680

Dave, S., Anghan, C., Saincher, S., & Banerjee, J. (2018). A high-resolution Navier–Stokes solver for direct numerical simulation of free shear flow. *Numerical Heat Transfer, Part B: Fundamentals*, *74*(6), 840–860. https://doi.org/10.1080/10407790.2019.1580952

Delandmeter, P., Lambrechts, J., Legat, V., Vallaeys, V., Naithani, J., Thiery, W., Remacle, J-F., & Deleersnijder, E. (2018). A fully consistent and conservative vertically adaptive coordinate system for SLIM 3D v0.4 with an application to the thermocline oscillations of Lake Tanganyika. *Geoscientific Model Development*, *11*(3), 1161-1179. https://doi.org/10.5194/gmd-11-1161-2018

Divya, R., & Sriram, V. (2017). Wave-porous structure interaction modelling using Improved Meshless Local Petrov Galerkin method. *Applied Ocean Research*, *67*, 291–305. https://doi.org/10.1016/j.apor.2017.07.017

Divya, R., Sriram, V., & Murali, K. (2020). Wave-vegetation interaction using Improved Meshless Local Petrov Galerkin method. *Applied Ocean Research*, *101*, 102116. https://doi.org/10.1016/j.apor.2020.102116

Dommermuth, D. G., & Yue, D. K. P. (1987). A high-order spectral method for the study of nonlinear gravity waves. *Journal of Fluid Mechanics*, *184*, 267–288. https://doi.org/10.1017/s002211208700288x

Dommermuth, D. G. (1993). The laminar interactions of a pair of vortex tubes with a free surface. *Journal of Fluid Mechanics*, *246*, 91–115. https://doi.org/10.1017/s0022112093000059

Dong, W., Liu, J., Xie, Z., & Dong, L. (2019). Adaptive neural network-based approximation to accelerate eulerian fluid simulation. *SC '19: Proceedings of the International Conference for High Performance Computing, Networking, Storage and Analysis*. https://doi.org/10.1145/3295500.3356147

Drevard, D., Marcer, R., Grilli, S. T., Asce, M., Fraunié, P., & Rey, V. (2005). EXPERIMENTAL VALIDATION OF A COUPLED BEM-NAVIER-STOKES MODEL FOR SOLITARY WAVE SHOALING AND BREAKING. *Ocean Wave Measurement and Analysis: Fifth International Symposium, WAVES 2005 : 3rd - 7th July 2005, Madrid, Spain*. http://www.oce.uri.edu/~grilli/DMGFR-166_WAVES05.pdf

Drikakis, D., & Rider, W. J. (2005). High-Resolution methods for incompressible and Low-Speed flows. In *Springer eBooks*. https://doi.org/10.1007/b137615

Edmund, D. O., Maki, K. J., & Beck, R. F. (2013). A velocity-decomposition formulation for the incompressible Navier–Stokes equations. *Computational Mechanics*, *52*(3), 669–680. https://doi.org/10.1007/s00466-013-0839-6

Ferrant, P., Gentaz, L., & Touzé, D. L. (2002). A new RANSE/Potential Approach for Water Wave Diffraction. *Numerical Towing Tank Symposium, NuTTS'2002. At: Pornichet, France*. https://hal.science/hal-01155923

Ferziger, J. H., Perić, M., & Street, R. L. (2020). Computational methods for fluid dynamics. In *Springer eBooks*. https://doi.org/10.1007/978-3-319-99693-6

Fujima, K., Masamura, K., & Goto, C. (2002). DEVELOPMENT OF THE 2D/3D HYBRID MODEL FOR TSUNAMI NUMERICAL SIMULATION. *Coastal Engineering Journal*, *44* (4), 373-397. https://doi.org/10.1142/S0578563402000615

Gentaz, L., Luquet, R., Alessandrini, B., & Ferrant, P. (2004). Numerical simulation of the 3D viscous flow around a vertical cylinder in Non-Linear waves using an explicit incident wave model. *23rd International Conference on Offshore Mechanics and Arctic Engineering, Volume 1, Parts a and B*. https://doi.org/10.1115/omae2004-51098

Gilbert, R. W., Zedler, E. A., Grilli, S. T., & Street, R. L. (2007). Progress on Nonlinear-Wave-Forced Sediment Transport Simulation. *IEEE Journal of Oceanic Engineering*, *32*(1), 236–248. https://doi.org/10.1109/joe.2007.890979

Gong, J., Yan, S., Ma, Q., & Li, Y. (2020). Added resistance and seakeeping performance of trimarans in oblique waves. *Ocean Engineering*, *216*, 107721. https://doi.org/10.1016/j.oceaneng.2020.107721

Greco, M. (2001). A Two-dimensional Study of Green-Water Loading. Ph. D. thesis, Dept. Marine Hydrodynamics, NTNU, Trondheim, Norway. http://hdl.handle.net/11250/231252

Greco, M., Colicchio, G., & Faltinsen, O. M. (2007). Shipping of water on a two-dimensional structure. Part 2. *Journal of Fluid Mechanics*, *581*, 371–399. https://doi.org/10.1017/s002211200700568x

Green, A. E., & Naghdi, P. M. (1976). A derivation of equations for wave propagation in water of variable depth. *Journal of Fluid Mechanics*, *78*(2), 237-246. https://doi.org/10.1017/S0022112076002425

Grilli, S. T., & Horrillo, J. (1999). Shoaling of periodic waves over Barred-Beaches in a fully nonlinear numerical wave tank. *International Journal of Offshore and Polar Engineering*, *9*(04), 257–263. https://ci.nii.ac.jp/naid/10025319120

Grilli, S. T. & Horrillo, J. (1997). Numerical generation and absorption of fully nonlinear periodic waves. *Journal of Engineering Mechanics*, *123(10)*, 1060-1069. https://doi.org/10.1061/(ASCE)0733-9399(1997)123:10(1060)

Grilli, S. T., Guyenne, P. & Dias, F. (2001). A fully non-linear model for three-dimensional overturning waves over an arbitrary bottom. *International Journal for Numerical Methods in Fluids*, *35*, 829-867. https://doi.org/10.1002/1097-0363(20010415)35:7%3C829::AID-FLD115%3E3.0.CO;2-2

Grilli, S. T., Gilbert, R. W., Lubin, P., Vincent, S., Astruc, D., Legendre, D., Duval, M., Kimmoun, O., Branger, H., Devrard, D., Fraunié, P., & Abadie, S. (2004). Numerical modeling and experiments for solitary wave shoaling and breaking over a sloping beach. *HAL (Le Centre Pour La Communication Scientifique Directe)*. https://hal.science/hal-00084408

Grilli, S. T., Harris, J. C., & Greene, N. (2009). MODELING OF WAVE-INDUCED SEDIMENT TRANSPORT AROUND OBSTACLES. *Proceedings of the 31st International Conference, Hamburg, Germany, 31 August – 5 September 2008*. https://doi.org/10.1142/9789814277426_0136

Grilli, S. T., Dias, F., Guyenne, P., Fochesato, C., & Enet, F. (2010). PROGRESS IN FULLY NONLINEAR POTENTIAL FLOW MODELING OF 3D EXTREME OCEAN WAVES. In *WORLD SCIENTIFIC eBooks* (pp. 75–128). https://doi.org/10.1142/9789812836502_0003

Hafsia, Z., Hadj, M. B., Lamloumi, H., & Maalel, K. (2009). Internal inlet for wave generation and absorption treatment. *Coastal Engineering*, *56*(9), 951–959. https://doi.org/10.1016/j.coastaleng.2009.05.001

Haidvogel, D. B., Arango, H., Budgell, W. P., Cornuelle, B. D., Curchitser, E., Di Lorenzo, E., Fennel, K., Geyer, W. R., Hermann, A. J., Lanerolle, L., Levin, J., McWilliams, J. C., Miller, A. J., Moore, A. M., Powell, T. M., Shchepetkin, A. F., Sherwood, C. R., Signell, R. P., Warner, J. C., & Wilkin, J. (2008). Ocean forecasting in terrain-following coordinates: Formulation and skill assessment of the Regional Ocean Modeling System. *Journal of Computational Physics*, *227*, 3595-3624. https://doi.org/10.1016/j.jcp.2007.06.016

Hanert, E., Mohammed, A. V., Veerasingam, S., Dobbelaere, T., Vallaeys, V., & Vethamony, P. (2023). A multiscale ocean modelling system for the central Arabian/Persian Gulf: From regional to structure scale circulation patterns. *Estuarine, Coastal and Shelf Science*, *282*, 108230. https://doi.org/10.1016/j.ecss.2023.108230

Hasan, S., Sriram, V., & Selvam, R. P. (2019). Evaluation of an eddy viscosity type wave breaking model for intermediate water depths. *European Journal of Mechanics - B/Fluids*, *78*, 115–138. https://doi.org/10.1016/j.euromechflu.2019.06.005

Hildebrandt, A., Sriram, V., & Schlurmann, T. (2013). Simulation of focusing waves and local line forces due to wave impacts on a tripod structure. *The Twenty-third International Offshore and Polar Engineering Conference*. https://onepetro.org/ISOPEIOPEC/proceedings/ISOPE13/All-ISOPE13/ISOPE-I-13-359/15498

Jacobsen, N. G., Fuhrman, D. R., & Fredsøe, J. (2011). A wave generation toolbox for the open-source CFD library: OpenFoam®. *International Journal for Numerical Methods in Fluids*, *70*(9), 1073–1088. https://doi.org/10.1002/fld.2726

Kassiotis, C., Ferrand, M., Violeau, D., Rogers, B. D., Stansby, P., & Benoît, M. (2011). Coupling SPH with a 1-D Boussinesq-type wave model. *HAL (Le Centre Pour La Communication Scientifique Directe)*. https://hal-enpc.archives-ouvertes.fr/hal-00601352

Kim, C., Clément, A., & Tanizawa, K. (1999). Recent research and development of Numerical Wave Tank - a review. *HAL (Le Centre Pour La Communication Scientifique Directe)*. https://hal.science/hal-00699394

Kim, K., Sirviente, A. I., & Beck, R. F. (2005). The complementary RANS equations for the simulation of viscous flows. *International Journal for Numerical Methods in Fluids*, *48*(2), 199–229. https://doi.org/10.1002/fld.892

Kim, Y. J. (2021). Numerical improvement and validation of a naval hydrodynamics CFD solver in view of performing fast and accurate simulation of complex ship-wave interaction. Ph.D. thesis. École centrale de Nantes. https://theses.hal.science/tel-03530266

Kumar, G. M., Sriram, V., & Didenkulova, I. (2020). A hybrid numerical model based on FNPT-NS for the estimation of long wave run-up. *Ocean Engineering*, *202*, 107181. https://doi.org/10.1016/j.oceaneng.2020.107181

Kumar, G. M., & Sriram, V. (2020). Development of a hybrid model based on mesh and meshfree methods and its application to fluid–elastic structure interaction for free surface waves. *Journal of Fluids and Structures*, *99*, 103159. https://doi.org/10.1016/j.jfluidstructs.2020.103159

Kutz, J. N. (2017). Deep learning in fluid dynamics. *Journal of Fluid Mechanics*, *814*, 1–4. https://doi.org/10.1017/jfm.2016.803

Lachaume, C., Biausser, B., Grilli, S. T., Fraunié, P., & Guignard, S. (2003). Modeling of breaking and post-breaking waves on slopes by coupling of BEM and VOF methods. *The Thirteenth International Offshore and Polar Engineering Conference*, 1698. http://personal.egr.uri.edu/grilli/3053p353.pdf

Ladický, Ľ., Jeong, S., Solenthaler, B., Pollefeys, M., & Groß, M. (2015). Data-driven fluid simulations using regression forests. *ACM Transactions on Graphics*, *34*(6), 1–9. https://doi.org/10.1145/2816795.2818129

Larsen, B., & Fuhrman, D. R. (2018). On the over-production of turbulence beneath surface waves in Reynolds-averaged Navier–Stokes models. *Journal of Fluid Mechanics*, *853*, 419–460. https://doi.org/10.1017/jfm.2018.577

Li, Z., Bouscasse, B., Gentaz, L., Ducrozet, G., & Ferrant, P. (2018). Progress in Coupling Potential Wave Models and Two-Phase Solvers With the SWENSE Methodology. *ASME 2018 37th International Conference on Ocean, Offshore and Arctic Engineering. June 17–22, 2018 Madrid, Spain*. https://doi.org/10.1115/omae2018-77466

Li, Q., Wang, J., Yan, S., Gong, J., & Ma, Q. (2018). A zonal hybrid approach coupling FNPT with OpenFOAM for modelling wave-structure interactions with action of current. *Ocean Systems Engineering*, *8*(4), 381–407. https://doi.org/10.12989/ose.2018.8.4.381

Li, Z., Bouscasse, B., Ducrozet, G., Gentaz, L., Touzé, D. L., & Ferrant, P. (2021). Spectral Wave Explicit Navier-Stokes Equations for wave-structure interactions using two-phase Computational Fluid Dynamics solvers. *Ocean Engineering*, *221*, 108513. https://doi.org/10.1016/j.oceaneng.2020.108513

Li, Q., Yan, S., Zhang, Y., Zhang, N., Ma, Q., & Xie, Z. (2023). Numerical Modelling of Breaking Wave Impacts on Seawalls with Recurved Parapets Using qaleFOAM. *International Journal of Offshore and Polar Engineering*, *33*(2), 157–163. https://doi.org/10.17736/ijope.2023.sv05

Lin, P., & Liu, P. L. (1998). A numerical study of breaking waves in the surf zone. *Journal of Fluid Mechanics*, *359*, 239–264. https://doi.org/10.1017/s002211209700846x

Lin, P., & Liu, P. L. (1999). Internal Wave-Maker for Navier-Stokes Equations Models. *Journal of Waterway, Port, Coastal, and Ocean Engineering*, *125*(4), 207–215. https://doi.org/10.1061/(ASCE)0733-950X(1999)125:4(207)

Lind, S., Rogers, B. D., & Stansby, P. (2020). Review of smoothed particle hydrodynamics: towards converged Lagrangian flow modelling. *Proceedings of the Royal Society A: Mathematical, Physical and Engineering Sciences*, *476*(2241). https://doi.org/10.1098/rspa.2019.0801

Ling, J., Kurzawski, A., & Templeton, J. A. (2016). Reynolds averaged turbulence modelling using deep neural networks with embedded invariance. *Journal of Fluid Mechanics*, *807*, 155–166. https://doi.org/10.1017/jfm.2016.615

Longuet-Higgins, M. S., & Cokelet, E. D. (1976). The deformation of steep surface waves on water - I. A numerical method of computation. *Proceedings of the Royal Society of London*, *350*(1660), 1–26. https://doi.org/10.1098/rspa.1976.0092

Luo, M., Khayyer, A., & Lin, P. (2021). Particle methods in ocean and coastal engineering. *Applied Ocean Research*, *114*, 102734. https://doi.org/10.1016/j.apor.2021.102734

Luquet, R., Ferrant, P., Alessandrini, B., Ducrozet, G., & Gentaz, L. (2007). Simulation of a TLP in Waves using the SWENSE Scheme. *HAL (Le Centre Pour La Communication Scientifique Directe)*. https://hal.archives-ouvertes.fr/hal-01156200

Lynett, P. J., Wu, T-R., & Liu, P. L-. F. (2002). Modeling wave runup with depth-integrated equations. *Coastal Engineering*, *46*(2), 89-107. https://doi.org/10.1016/S0378-3839(02)00043-1

Lynett, P. J., & Liu, P. L-. F. (2004a). Linear analysis of the multi-layer model. *Coastal Engineering*, *51*, 439-454. https://doi.org/10.1016/j.coastaleng.2004.05.004

Lynett, P. J., & Liu, P. L. -F. (2004b). A two-layer approach to wave modelling. *Proceedings of the Royal Society A: Mathematical, Physical and Engineering Sciences*, *460*, 2637-2669. https://doi.org/10.1098/rspa.2004.1305

Ma, Q. W. (2005). Meshless local Petrov–Galerkin method for two-dimensional nonlinear water wave problems. *Journal of Computational Physics*, *205*(2), 611–625. https://doi.org/10.1016/j.jcp.2004.11.010

Ma, Q. W. (2008). A new meshless interpolation scheme for MLPG_R method. *CMES-computer Modeling in Engineering & Sciences*, *23*(2), 75–90. https://doi.org/10.3970/cmes.2008.023.075

Ma, Q. W., & Yan, S. (2008). QALE-FEM for numerical modelling of non-linear interaction between 3D moored floating bodies and steep waves. *International Journal for Numerical Methods in Engineering*, *78*(6), 713–756. https://doi.org/10.1002/nme.2505

Ma, Q. W., & Zhou, J. (2009). MLPG_R Method for Numerical Simulation of 2D breaking waves. *CMES-computer Modeling in Engineering & Sciences*, *43*(3), 277–304. https://doi.org/10.3970/cmes.2009.043.277

Madsen, P. A., Murray, R., & Sørensen, O. R. (1991). A new form of the Boussinesq equations with improved linear dispersion characteristics. *Coastal Engineering*, *15*(4), 371-388. https://doi.org/10.1016/0378-3839(91)90017-B

Madsen, P. A., Bingham, H. B., & Liu, H. (2002). A new Boussinesq method for fully nonlinear waves from shallow to deep water. *Journal of Fluid Mechanics*, *462*, 1-30. https://doi.org/10.1017/S0022112002008467

Mellor, G. L., & Yamada, T. (1982). Development of a turbulence closure model for geophysical fluid problems. *Reviews of Geophysics*, *20*(4), 851-875. https://doi.org/10.1029/RG020i004p00851

Mohanlal, S. (2023). Improvement of the 2D and 3D modeling of breaking waves in a maritime environment. Doctoral dissertation, École des Ponts ParisTech. https://pastel.hal.science/tel-04526480v1/document

Monroy, C., Ducrozet, G., Bonnefoy, F., Babarit, A., Gentaz, L., & Ferrant, P. (2010). RANS Simulations of CALM Buoy In Regular And Irregular Seas Using SWENSE Method. *International Journal of Offshore and Polar Engineering*, *21*(4). https://onepetro.org/IJOPE/article-abstract/35598/RANS-Simulations-of-CALM-Buoy-In-Regular-And?redirectedFrom=PDF

Narayanaswamy, M., Crespo, A., Gómez-Gesteira, M., & Dalrymple, R. A. (2010). SPHysics-FUNWAVE hybrid model for coastal wave propagation. *Journal of Hydraulic Research*, *48*(sup1), 85–93. https://doi.org/10.1080/00221686.2010.9641249

Nwogu, O. (1993). Alternative Form of Boussinesq Equations for Nearshore Wave Propagation. *Journal of Waterway, Port, Coastal, and Ocean Engineering*, *119*(6), 618-638. https://doi.org/10.1061/(ASCE)0733-950X(1993)119:6(618)

O'Shea, T. T., Brucker, K. A., Dommermuth, D. G., & Wyatt, D. C. (2014). A numerical formulation for simulating Free-Surface hydrodynamics. *arXiv (Cornell University)*. https://arxiv.org/pdf/1410.2240.pdf

Peregrine, D. H. (1967). Long waves on a beach. *Journal of Fluid Mechanics*, *27*(4), 815-827. https://doi.org/10.1017/S0022112067002605

Qu, K., Tang, H. S., Agrawal, A., Jiang, C. B., & Deng, B. (2016). Evaluation of SIFOM-FVCOM system for high-fidelity simulation of small-scale coastal ocean flows. *Journal of Hydrodynamics*, *28*(6), 994-1002. https://doi.org/10.1016/S1001-6058(16)60701-1

Qu, K., Sun, W. Y., Tang, H. S., Jiang, C. B., Deng, B., & Chen, J. (2019a). Numerical study on hydrodynamic load of real-world tsunami wave at highway bridge deck using a coupled modeling system. *Ocean Engineering*, *192*, 106486. https://doi.org/10.1016/j.oceaneng.2019.106486

Qu, K., Tang, H. S., & Agrawal, A. (2019b). Integration of fully 3D fluid dynamics and geophysical fluid dynamics models for multiphysics coastal ocean flows: Simulation of local complex free-surface phenomena. *Ocean Modelling*, *135*, 14-30. https://doi.org/10.1016/j.ocemod.2019.01.001

Raissi, M., Yazdani, A., & Karniadakis, G. E. (2020). Hidden fluid mechanics: Learning velocity and pressure fields from flow visualizations. *Science*, *367*(6481), 1026–1030. https://doi.org/10.1126/science.aaw4741

Ransley, E., Yan, S., Brown, S., Mai, T., Graham, D. I., Ma, Q., Musiedlak, P., Engsig-Karup, . . . Greaves, D. (2019). A Blind Comparative Study of Focused Wave Interactions with a Fixed FPSO-like Structure (CCP-WSI Blind Test Series 1). *International Journal of Offshore and Polar Engineering*, *29*(2), 113–127. https://doi.org/10.17736/ijope.2019.jc748

Ransley, E., Yan, S., Brown, S., Hann, M., Graham, D. I., Windt, C., Schmitt, P., Davidson, J., . . . Greaves, D. (2020). A Blind Comparative Study of Focused Wave Interactions with Floating Structures (CCP-WSI Blind Test Series 3). *International Journal of Offshore and Polar Engineering*, *30*(1), 1–10. https://doi.org/10.17736/ijope.2020.jc774

Rijas, A. S., & Sriram, V. (2019). Numerical modelling of forced heaving of mono hull and twin hull in particle method. *Ocean Engineering*, *173*, 197–214. https://doi.org/10.1016/j.oceaneng.2018.12.066

Rijas, A. S., Sriram, V., & Yan, S. (2019). Variable spaced particle in mesh-free method to handle wave-floating body interactions. *International Journal for Numerical Methods in Fluids*, *91*(6), 263–286. https://doi.org/10.1002/fld.4751

Robaux, F. (2020). Numerical simulation of wave-body interaction: development of a fully nonlinear potential flow solver and assessment of two local coupling strategies with a CFD solver. Ph.D. thesis. Université Aix Marseille. https://theses.hal.science/tel-03515567/

Robaux, F., & Benoît, M. (2021). Development and validation of a numerical wave tank based on the Harmonic Polynomial Cell and Immersed Boundary methods to model nonlinear wave-structure interaction. *Journal of Computational Physics*, *446*, 110560. https://doi.org/10.1016/j.jcp.2021.110560

Rodi, W., Constantinescu, G., & Stoesser, T. (2013). Large-Eddy simulation in hydraulics. In *CRC Press eBooks*. https://doi.org/10.1201/b15090

Rosemurgy, W. J., Beck, R. F., & Maki, K. J. (2016). A velocity decomposition formulation for 2D steady incompressible lifting problems. *European Journal of Mechanics - B/Fluids*, *58*, 70–84. https://doi.org/10.1016/j.euromechflu.2016.03.007

Saincher, S., & Banerjee, J. (2015). A Redistribution-Based Volume-Preserving PLIC-VOF technique. *Numerical Heat Transfer, Part B: Fundamentals*, *67*(4), 338–362. https://doi.org/10.1080/10407790.2014.950078

Saincher, S., & Banerjee, J. (2017a). A volume-preserving inflow boundary based numerical tank applied to wave-structure interaction in near-shallow water, *Proceedings of the 7^{th} International Conference on Computational Methods in Marine Engineering* (MARINE 2017 - held at Nantes, France). http://hdl.handle.net/2117/332048

Saincher, S., & Banerjee, J. (2017b). On wave damping occurring during source-based generation of steep waves in deep and near-shallow water. *Ocean Engineering*, *135*, 98–116. https://doi.org/10.1016/j.oceaneng.2017.03.003

Saincher, S., & Banerjee, J. (2018). Two-Phase Navier-Stokes Simulations of Plunging Breaking Waves, *Proceedings of the 7th International and 45th National Conference on Fluid Mechanics and Fluid Power* (FMFP 2018 - held at IIT Bombay, India).

Saincher, S., Sriram, V., & Didenkulova, I. (2021). Run-up of breaking focused waves on a beach studied experimentally in a large scale facility and numerically using hybrid FNPT-RANS model, EGU General Assembly 2021, online, 19–30 Apr 2021, EGU21-14148. https://doi.org/10.5194/egusphere-egu21-14148

Saincher, S., & Sriram, V. (2022a). An efficient operator-split CICSAM scheme for three-dimensional multiphase-flow problems on Cartesian grids. *Computers & Fluids*, *240*, 105440. https://doi.org/10.1016/j.compfluid.2022.105440

Saincher, S., & Sriram, V. (2022b). A three dimensional hybrid fully nonlinear potential flow and Navier Stokes model for wave structure interactions. *Ocean Engineering*, *266*, 112770. https://doi.org/10.1016/j.oceaneng.2022.112770

Saincher, S., & Sriram, V. (2023). Comparative assessment of non-conservative and conservative RANS formulations for coastal applications involving breaking waves. *Coastal Engineering Proceedings*, *37*, 33. https://doi.org/10.9753/icce.v37.papers.33

Saincher, S., Sriram, V., Ravindar, R., Yan, S., Stagonas, D., . . . Wan, D. (2023a). Comparative Study on Breaking Waves Interaction with Vertical Wall Retrofitted with Recurved Parapet in Small and Large Scale. *International Journal of Offshore and Polar Engineering*, *33*(2), 113–122. https://doi.org/10.17736/ijope.2023.jc890

Saincher, S., Srivastava, K., Vijayakumar, R., & Sriram, V. (2023b). Application of IITM-RANS3D to free-fall water entry of prismatic and non-prismatic finite wedges. *Journal of Hydrodynamics*, *35*(3), 417–430. https://doi.org/10.1007/s42241-023-0040-0

Shchepetkin, A. F. & McWilliams, J. C. (2005). The regional oceanic modeling system (ROMS): a split-explicit, free-surface, topography-following-coordinate oceanic model. *Ocean Modelling*, *9*, 347-404. https://doi.org/10.1016/j.ocemod.2004.08.002

Seiffert, B. R., & Ducrozet, G. (2018). Simulation of breaking waves using the high-order spectral method with laboratory experiments: wave-breaking energy dissipation. *Ocean Dynamics*, *68*(1), 65–89. https://doi.org/10.1007/s10236-017-1119-3

Sharma, A. (2022). Introduction to computational fluid dynamics. In *Springer eBooks*. https://doi.org/10.1007/978-3-030-72884-7

Shi, F., Kirby, J. T., Harris, J. C., Geiman, J. D., & Grilli, S. T. (2012). A high-order adaptive time-stepping TVD solver for Boussinesq modeling of breaking waves and coastal inundation. *Ocean Modelling*, *43–44*, 36–51. https://doi.org/10.1016/j.ocemod.2011.12.004

Sitanggang, K. I., & Lynett, P. (2005). Parallel computation of a highly nonlinear Boussinesq equation model through domain decomposition. *International Journal for Numerical Methods in Fluids*, *49*, 57-74. https://doi.org/10.1002/fld.985

Sitanggang, K. I., & Lynett, P. J. (2010). Multi-scale simulation with a hybrid Boussinesq-RANS hydrodynamic model. *International Journal for Numerical Methods in Fluids*, *62*, 1013-1046. https://doi.org/10.1002/fld.2056

Sriram, V., & Ma, Q. W. (2012). Improved MLPG_R method for simulating 2D interaction between violent waves and elastic structures. *Journal of Computational Physics*, *231*(22), 7650–7670. https://doi.org/10.1016/j.jcp.2012.07.003

Sriram, V., Ma, Q. W., & Schlurmann, T. (2014). A hybrid method for modelling two dimensional non-breaking and breaking waves. *Journal of Computational Physics*, *272*, 429–454. https://doi.org/10.1016/j.jcp.2014.04.030

Sriram, V., & Ma, Q. W. (2021). Review on the local weak form-based meshless method (MLPG): Developments and Applications in Ocean Engineering. *Applied Ocean Research*, *116*, 102883. https://doi.org/10.1016/j.apor.2021.102883

Sriram, V., Agarwal, S., Yan, S., Xie, Z., Saincher, S., Schlurmann, T., Ma, Q., . . . Li, G. (2021). A comparative study on the nonlinear interaction between a focusing wave and cylinder using state-of-the-art solvers: Part A. *International Journal of Offshore and Polar Engineering*, *31*(1), 1–10. https://doi.org/10.17736/ijope.2021.jc820

Tafti, D. K. (1996). Comparison of some upwind-biased high-order formulations with a second-order central-difference scheme for time integration of the incompressible Navier-Stokes equations. *Computers & Fluids*, *25*(7), 647–665. https://doi.org/10.1016/0045-7930(96)00015-1

Tang, H. S., Qu, K., & Wu, X. G. (2014). An overset grid method for integration of fully 3D fluid dynamics and geophysics fluid dynamics models to simulate multiphysics coastal ocean flows. *Journal of Computational Physics*, *273*, 548-571. https://doi.org/10.1016/j.jcp.2014.05.010

Tanizawa, K., & Clément, A. (2000). Report of the 2nd Workshop of ISOPE Numerical Wave Tank Group:Benchmark Test Cases of Radiation Problem, (Brest, May 1999). *Proceedings of the 10th International Offshore and Polar Engineering Conference, Seattle, Washington, USA, May 2000.* https://onepetro.org/ISOPEIOPEC/proceedings-abstract/ISOPE00/All-ISOPE00/ISOPE-I-00-242/7146

Tian, Z., Perlin, M., & Choi, W. (2010). Energy dissipation in two-dimensional unsteady plunging breakers and an eddy viscosity model. *Journal of Fluid Mechanics*, *655*, 217–257. https://doi.org/10.1017/s0022112010000832

Tompson, J., Schlachter, K., Sprechmann, P., & Perlin, K. (2016). Accelerating eulerian fluid simulation with convolutional networks. *arXiv (Cornell University)*. https://doi.org/10.48550/arxiv.1607.03597

Tryggvason, G., Sussman, M., & Hussaini, M. Y. (2007). Immersed boundary methods for fluid interfaces. In A. Prosperetti & G. Tryggvason (Eds.), Computational Methods for Multiphase Flow (pp. 37–77). chapter, Cambridge: Cambridge University Press. https://doi.org/10.1017/CBO9780511607486

Vineesh, P., & Sriram, V. (2023). Numerical investigation of wave interaction with two closely spaced floating boxes using particle method. *Ocean Engineering*, *268*, 113465. https://doi.org/10.1016/j.oceaneng.2022.113465

Wei, G., Kirby, J. T., Grilli, S. T., & Subramanya, R. (1995). A fully nonlinear Boussinesq model for surface waves. Part 1. Highly nonlinear unsteady waves. *Journal of Fluid Mechanics*, 294, 71-92. https://doi.org/10.1017/S0022112095002813

Wessels, H., Weißenfels, C., & Wriggers, P. (2020). The neural particle method – An updated Lagrangian physics informed neural network for computational fluid dynamics. *Computer Methods in Applied Mechanics and Engineering*, *368*, 113127. https://doi.org/10.1016/j.cma.2020.113127

West, B. J., Brueckner, K. A., Janda, R., Milder, D. M., & Milton, R. L. (1987). A new numerical method for surface hydrodynamics. *Journal of Geophysical Research*, *92*(C11), 11803–11824. https://doi.org/10.1029/jc092ic11p11803

Xiao, X., Zhou, Y., Wang, H., & Yang, X. (2020). A novel CNN-Based poisson solver for fluid simulation. *IEEE Transactions on Visualization and Computer Graphics*, *26*(3), 1454–1465. https://doi.org/10.1109/tvcg.2018.2873375

Xiao, Q., Calvert, R., Yan, S., Adcock, T. A. A., & Van Den Bremer, T. S. (2024). Surface gravity wave-induced drift of floating objects in the diffraction regime. *Journal of Fluid Mechanics*, *980*. https://doi.org/10.1017/jfm.2024.31

Xie, Z., & Stoesser, T. (2020). Two-phase flow simulation of breaking solitary waves over surface-piercing and submerged conical structures. *Ocean Engineering*, *213*, 107679. https://doi.org/10.1016/j.oceaneng.2020.107679

Xie, Z., & Stoesser, T. (2023). Turbulence Structure due to Wave-Vegetation Interaction. In *WORLD SCIENTIFIC eBooks* (pp. 179–202). https://doi.org/10.1142/9789811284144_0008

Yan, S., W, Q., Wang, J., & Zhou, J. (2016). Self-Adaptive Wave Absorbing Technique for Nonlinear Shallow Water Waves. *ASME 2016 35th International Conference on Ocean, Offshore and Arctic Engineering*. https://doi.org/10.1115/omae2016-54475

Yan, S., Wang, J., Wang, J., Ma, Q., & Xie, Z. (2020). CCP-WSI Blind Test Using qaleFOAM with an Improved Passive Wave Absorber. *International Journal of Offshore and Polar Engineering*, *30*(1), 43–52. https://doi.org/10.17736/ijope.2020.jc781

Yang, C., Yang, X., & Xiao, X. (2016). Data-driven projection method in fluid simulation. *Computer Animation and Virtual Worlds*, *27*(3–4), 415–424. https://doi.org/10.1002/cav.1695

Yang, Z. T., & Liu, P. L. -F. (2020). Depth-integrated wave–current models. Part 1. Two-dimensional formulation and applications. *Journal of Fluid Mechanics*, 883. https://doi.org/10.1017/jfm.2019.831

Yang, Z., & Liu, P. L. -F. (2022). Depth-integrated wave–current models. Part 2. Current with an arbitrary profile. *Journal of Fluid Mechanics*, 936. https://doi.org/10.1017/jfm.2022.42

Yu, Z., Ma, Q., Zheng, X., Liao, K., Sun, H., & Khayyer, A. (2023). A hybrid numerical model for simulating aero-elastic-hydro-mooring-wake dynamic responses of floating offshore wind turbine. *Ocean Engineering*, *268*, 113050. https://doi.org/10.1016/j.oceaneng.2022.113050

Yuan, Y., Ma, Q., Yan, S., Zheng, X., Liao, K., Ma, G., Sun, H., & Khayyer, A. (2023). A hybrid method for modelling wake flow of a wind turbine. *Ocean Engineering*, *281*, 114770. https://doi.org/10.1016/j.oceaneng.2023.114770

Zhang, Z. J., & Duraisamy, K. (2015). Machine Learning Methods for Data-Driven Turbulence Modeling. *22nd AIAA Computational Fluid Dynamics Conference*. https://doi.org/10.2514/6.2015-2460

Zhang, N., Yan, S., Ma, Q., Guo, X., Xie, Z., & Zheng, X. (2023). A CNN-supported Lagrangian ISPH model for free surface flow. *Applied Ocean Research*, *136*, 103587. https://doi.org/10.1016/j.apor.2023.103587

Zhang, N., Yan, S., Ma, Q., & Li, Q. (2024a). A hybrid method combining ISPH with graph neural network for simulating free surface flows. *Computer Physics Communications*, *301*, 109220. https://doi.org/10.1016/j.cpc.2024.109220

Zhang, N., Yan, S., Ma, Q., & Li, Q. (2024b). Numerical simulation of wave-floater interaction using ISPH_GNN trained on data for wave-only cases. *Ocean Engineering*, *306*, 118041. https://doi.org/10.1016/j.oceaneng.2024.118041

Zhou, J., & Ma, Q. (2010). MLPG method based on Rankine Source solution for modelling 3D breaking waves. *CMES-computer Modeling in Engineering & Sciences*, *56*(2), 179–210. https://doi.org/10.3970/cmes.2010.056.179

Zhou, Y., Ma, Q., & Yan, S. (2016). MLPG_R method for modelling 2D flows of two immiscible fluids. *International Journal for Numerical Methods in Fluids*, *84*(7), 385–408. https://doi.org/10.1002/fld.4353

Zhou, Y., & Dong, P. (2018). A new implementation method of sharp interface boundary conditions for particle methods in simulating wave interaction with submerged porous structure. *Computers & Fluids*, *177*, 87–100. https://doi.org/10.1016/j.compfluid.2018.09.022

Zinjala, H. K., & Banerjee, J. (2016). A Lagrangian-Eulerian advection scheme with moment-of-fluid interface reconstruction. *Numerical Heat Transfer, Part B: Fundamentals*, *69*(6), 563–574. https://doi.org/10.1080/10407790.2016.1138753

Zinjala, H. K., & Banerjee, J. (2017). Refined moment-of-fluid method. *Numerical Heat Transfer, Part B: Fundamentals*, *71*(6), 574–591. https://doi.org/10.1080/10407790.2017.1309185

NOMENCLATURE

Roman symbols

$\vec{g}$	Gravitational acceleration vector
H	Wave-height
k	Turbulence kinetic energy
kd	Relative depth
L	Wavelength
$\mathcal{L}$	Characteristic length scale
p	Pressure in instantaneous NSE
p'	Modified pressure in time-averaged or filtered NSE
Re	Reynolds number
U ; V ; W	Components of $\vec{V}$ along the x, y and z directions respectively
U_{cyl}	Speed of the moving cylinder
$\mathcal{V}$	Characteristic velocity scale
$\vec{V}$	Instantaneous or Reynolds averaged velocity vector
t	Time
x ; y ; z	Cartesian coordinate directions

Greek symbols

Δx ; Δy ; Δz	Cell-sizes along the x, y and z directions respectively
$\boldsymbol{\varepsilon}$	Turbulence dissipation rate
$\boldsymbol{\eta}$	Free-surface elevation
$\boldsymbol{\mu}^*$	Mixture dynamic viscosity
$\boldsymbol{\mu_t}$	Turbulent or eddy viscosity
$\boldsymbol{\nu}$	Kinematic viscosity
$\boldsymbol{\rho}^*$	Mixture density
$\boldsymbol{\sigma}$	Topography-following vertical coordinate
$\boldsymbol{\phi}$	Velocity potential
$\boldsymbol{\omega}$	Specific dissipation rate

Superscripts

$\boldsymbol{Q}^*$	Predicted value of Q in a projection method
$\boldsymbol{Q}'$	Corrected value of Q in a projection method
$\boldsymbol{Q^n}$	Previous time-level value of Q
$\boldsymbol{Q^{n+1}}$	Current time-level value of Q

Abbreviations

ABM	Adams-Bashforth Method
ADI	Alternating Direction Implicit
AMM	Adams-Moulton Method
BBL	Bottom-Boundary Layer
BEM	Boundary Element Method
BiCGStab	Bi Conjugate Gradient Stabilized
BSNQE	Boussinesq Equations
CD	Central Difference
CFD	Computational Fluid Dynamics
CICSAM	Compressive Interface Capturing Scheme for Arbitrary Meshes
CNN	Convolution Neural Network
DD	Domain Decomposition
DNS	Direct Numerical Simulation
EOC	Equation Of Continuity
EOPC	Equation of Pressure Correction
EPBL	Energetically constrained Parameterization of the surface Boundary Layer
FD	Functional Decomposition
FDM	Finite Difference Method
FEBOUSS	Finite Element model for BOUSSinesq equations
FEM	Finite Element Method
FFD	Fast-Fictitious Domain
FiOU	Fifth Order Upwind
FNPT	Fully-Nonlinear Potential Theory
FOU	First Order Upwind
FOWT	Floating Offshore Wind Turbine
FVCOM	Finite Volume Coastal Ocean Model
FVM	Finite Volume Method
GFD	Geophysical Fluid Dynamics
GMRES	Generalized Minimal RESidual method

GNN	Graph Neural Network
GSSOR	Gauss-Seidel Successive Over-Relaxation
HOS	High-Order Spectral
HYCOM	HYbrid Coordinate Ocean Model
IITM-RANS3D	IIT Madras-RANS3D
IMLPG_R	Improved MLPG with Rankine source function
ILES	Implicit LES
ISPH	Incompressible SPH
KdV	Korteweg-De Vries
LBM	Lattice-Boltzmann Method
LES	Large-Eddy Simulation
LEAS-MOF	Lagrangian-Eulerian Advection Scheme-MOF
LMM	Linear Multi-step Method
MLD	Mixed Layer Depth
MLE	Mixed Layer Eddies
MLPG	Meshless Local Petrov-Galerkin
MOF	Moment Of Fluid
MOM	Modular Ocean Model
MPNDAF	Mixed Particle Number Density and Auxiliary Function
MPS	Moving Particle Semi-implicit
MSTACS	Modified Switching Technique for Advection and Capturing of Surfaces
NCOM	Navy Coastal Ocean Model
NITA	Non-Iterative Time Advancement
NFA	Numerical Flow Analysis
NS	Navier-Stokes
NSE	NS Equations
NWT	Numerical Wave Tank
OGCM	Ocean General Circulation Model
OS-CICSAM	Operator-Split CICSAM
PIMPLE	PISO-SIMPLE
PISO	Pressure-Implicit with Splitting of Operators
PLIC	Piecewise Linear Interface Calculation
POM	Princeton Ocean Model
PPE	Pressure Poisson Equation
QALE-FEM	Quasi-Arbitrary Lagrangian–Eulerian Finite Element Method
RANS	Reynolds-Averaged Navier Stokes
RANSE	RANS Equations
RK	Runge-Kutta
RMOF	Refined MOF
ROMS	Regional Oceanic Modeling System
RSM	Reynolds Stress Model
SAISH	Smoothly Adapting Interfacial Scheme based on Hybridization
SFDI	Simplified Finite Difference Interpolation
SGS	Sub-Grid-Scale
SIFOM	Solver for Incompressible Flow on Overset Meshes
SIFUM	Solver for Incompressible Flow on Unstructured Mesh
SIMPLE	Semi-Implicit Method for Pressure Linked Equations
SIS	Sea-Ice Simulator

SLIM	Second-generation Louvain-la-Neuve Ice-ocean Model
SOU	Second Order Upwind
SPH	Smoothed Particle Hydrodynamics
SWE	Shallow-Water Equations
SWENSE	Spectral Wave Explicit Navier Stokes Equations
TVD-RK	Total Variation Diminishing-RK
VOF	Volume Of Fluid
WALE	Wall-Adapting Local Eddy-viscosity
WENO	Weighted Essentially Non-Oscillatory
WSI	Wave-Structure Interaction